WAUo
59-28

DEPARTMENT OF
OCEANOGRAPHY
UNIVERSITY OF
WASHINGTON

Technical Report No. 62

THE DYNAMICS OF A FIORD ESTUARY:

SILVER BAY, ALASKA

by

William Bruce McAlister, Maurice Rattray, Jr.,
and Clifford A. Barnes

Office of Naval Research
Reference 59-28
November 1959

SEATTLE 5, WASHINGTON

UNIVERSITY OF WASHINGTON

DEPARTMENT OF OCEANOGRAPHY

Seattle 5, Washington

Technical Report No. 62

THE DYNAMICS OF A FIORD ESTUARY: SILVER BAY, ALASKA

by

William Bruce McAlister, Maurice Rattray, Jr.,
and Clifford A. Barnes

Office of Naval Research
Contract Nonr-477(10) and Nonr-477(01)

Reference 59-28
November 1959

RICHARD H. FLEMING
Executive Officer

Reproduction in whole or in part
is permitted for any purpose of the
United States Government.

ABSTRACT

Observations of water properties and movements made in July 1956 and March 1957, are used to describe the dynamics involved in the circulation of waters in Silver Bay, Alaska. This is an estuary system of a type commonly found along the coasts of British Columbia and Alaska, and the two seasons are representative of the extreme of summer and winter oceanographic conditions which occur in this locality.

In a tidal estuary, the addition of fresh water by river runoff produces mass and velocity fields in accordance with the principles of fluid mechanics. While the equations describing the distribution of mass and velocity are not solved in general, the individual terms in the equations are evaluated for Silver Bay, and their relative importance is assessed.

This procedure provides a quantitative description of the estuarine dynamics under the specific conditions observed, and allows a qualitative description of the effects of varying runoff and other conditions. With high runoff, and consequent large density gradients, it is found that the pressure gradient in the surface layers is largely balanced by the inertial terms; with low runoff, the pressure gradient balances the vertical stress gradient. The salt balance of the estuary is maintained primarily by advective processes. Previous theoretical work of Stommel and Cameron on the circulation in fiord estuaries is examined in view of the results obtained from Silver Bay.

TABLE OF CONTENTS

TABLE OF CONTENTS (continued)

LIST OF TABLES

LIST OF FIGURES

LIST OF SYMBOLS

A	Cross sectional area
f	Coriolis parameter
F_b	Bottom stress
F_{ij}	Components of molecular stress
g	Acceleration of gravity
k	Friction coefficient, also constant in stream function assumed by Cameron
N_z	Coefficient of eddy viscosity
p	Pressure
s	Salinity, concentration of dissolved salt
$\bar{s}$	Time mean salinity
s_m	Space mean salinity
S	Total salt content
T	Volume transport
t	Time
u_b	Bottom velocity
U	Tidal velocity
U_o	Amplitude of tidal velocity
V, v	Velocity
v_i	Instantaneous velocity in i-direction for respective coordinates
$\bar{v}_i$	Time mean velocity in i-direction
v_m	Space mean velocity of layer

(continued)

LIST OF SYMBOLS (continued)

v_i'	Instantaneous deviation from time mean velocity in i-direction
v_s	Surface velocity
$v_{x,z}$	Velocity in x-direction at depth z
X,Y,Z	Components of body forces
Δ, δ	Increment
ζ	Elevation above mean surface
ρ	Density
ρ_s	Surface density
ρ_b	Bottom density
σ_i	Surface element normal to i-direction
φ	Latitude
ω	Angular velocity of earth
$\doteq$	Approximates
$\langle\ \rangle$	Time average

CHAPTER 1

INTRODUCTION

1.1 Objectives of Study

The objective of this study is to describe the dynamics of the type of estuary system found in the deep inlets and fiords along the coast of Alaska and British Columbia. No thorough, well-documented exposition of the dynamics of circulation in such inlets is available. In this study the dynamics of the estuarine circulation is approached by setting up, as completely as possible, a set of equations; by using field data to evaluate the significance of the various measurable terms; and by computing numerically from the equations, using the measured quantities, the steady state distributions of those factors not readily measured. These measured and computed values should lead to a better understanding of the circulation, the nature of the forces involved in the mixing processes, and the dynamic structure of the estuary.

Pritchard (1954, 1956), using a similar approach in a study of Chesapeake Bay and James River data, has investigated in detail the salt balance, mixing processes, and dynamics of a coastal plain estuary. Ketchum (1951) and Stommel (1953) have studied the effects of tidal flushing and the circulation in vertically mixed estuaries.

Recent studies of fiord estuaries have been confined largely to the Canadian Pacific Coast. Tully (1949) has described the oceanography of Alberni Inlet and Nootka Sound. Pickard (1953, 1954) and Trites (1955) have described certain of the characteristics of inlets and fiords along the coast of British Columbia. Stommel (1952) and

Cameron (1951) have offered mathematical models to represent the circulations in fiords.

1.2 Definition and Classifications of Estuaries

A general definition which has gained wide acceptance is the one given by Pritchard (1952), who defines an estuary as "a semi-enclosed coastal body of water having a free connection with the open sea and containing a measurable quantity of sea salt." Estuaries are classified in terms of the relationship between evaporation and fresh water inflow and in terms of geomorphological structure.

Estuaries in which precipitation and fresh water inflow exceed evaporation, so as to produce a measurable dilution of sea water, are termed positive. When evaporation exceeds the combined total of precipitation and land drainage, the estuary is termed inverse. Neutral estuaries are those in which neither fresh water inflow nor evaporation predominate.

Further classification is made on the basis of geomorphological structure. Coastal plain estuaries are usually relatively shallow estuaries with dendritic shorelines formed by drowning of river valleys, either from subsidence of the land or from a rise in sea level. Bar-built estuaries result from the development of offshore bars in shallow water, on a shoreline of low relief. A third type of estuary is the deep basin or fiord, which has steep sides, a deep basin, and may or may not have a shallow sill at the mouth. This investigation is concerned primarily with the physical structure and circulation in fiord estuaries of the positive type.

1.3 Silver Bay

The data used in this study were obtained from Silver Bay, located on Baranof Island near Sitka, Alaska (Figure 1). Silver Bay is a fiord estuary of the positive type, is U-shaped, and ranges from one-half to three-fourths of a mile wide over most of its length. It extends approximately five miles from its confluence with Eastern Channel. There is no entrance sill, but a small sill at 35 fathoms is found one mile inside the mouth of Silver Bay proper. Midchannel depths in the main basin of Silver Bay average about 40 fathoms (Figure 2). Eastern Channel of Sitka Sound represents a seaward extension of the bay of approximately six miles, varying from one to three miles in width. Depths in Eastern Channel increase from about 60 fathoms near the head to 70 fathoms, present throughout most of the channel.

Oceanographic investigations were undertaken in Silver Bay in 1956 and 1957, in part to obtain basic information pertinent to predicting the movement and dispersion therein of waste liquor from a proposed pulp-mill scheduled for construction at the mouth of Sawmill Creek (Medvetcha River). The hydrography, geology, and biology of Silver Bay were investigated and detailed bathymetric charts of Silver Bay were prepared.

1.4 General Distribution of Properties

The currents in Silver Bay are oscillatory in nature, following the tides, and a net non-tidal circulation exists. It is this circulation which is associated with the observed distribution of properties. During the late spring and summer period of high runoff, a surface layer of

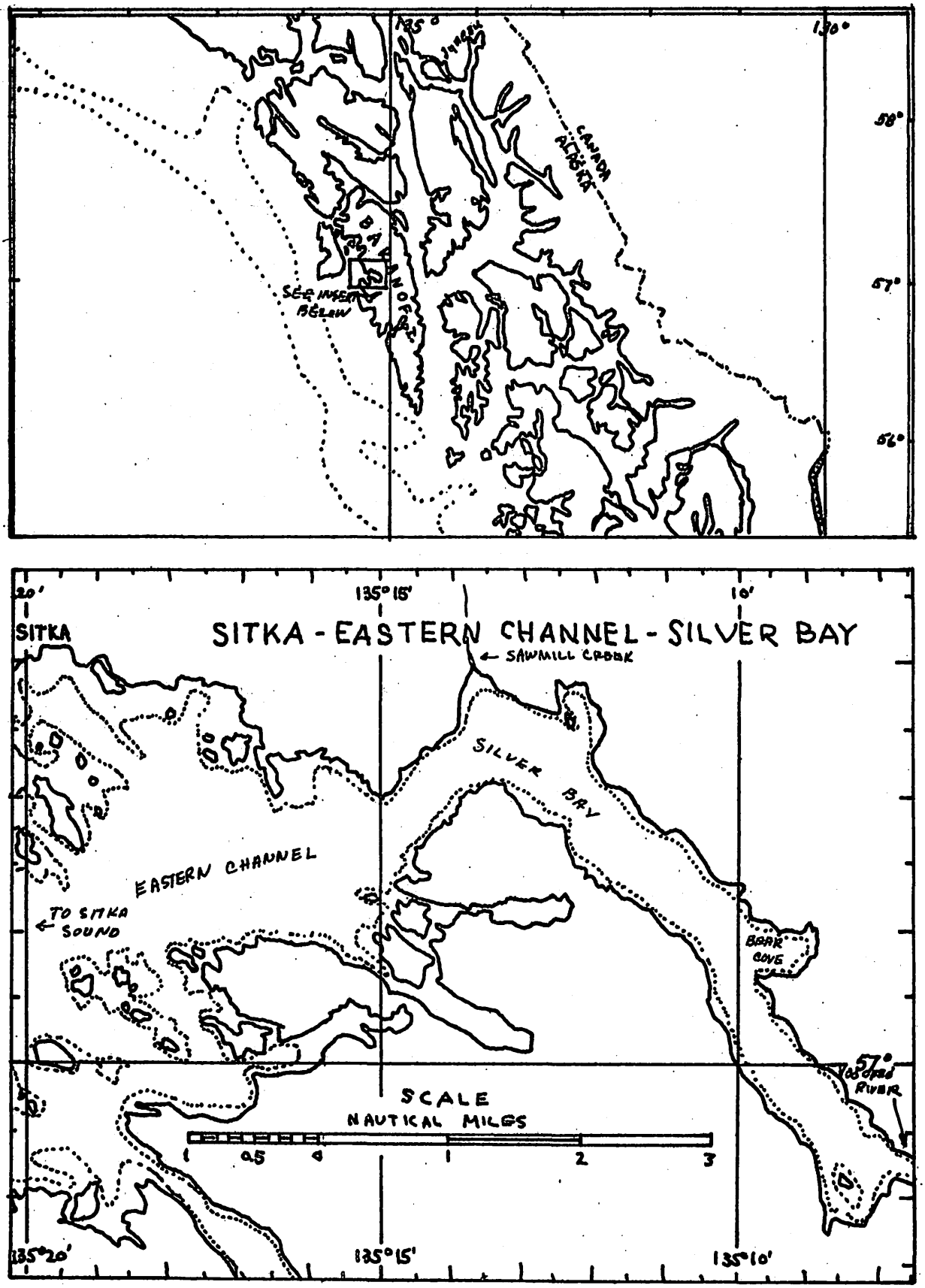

Figure 1. Silver Bay and Approaches

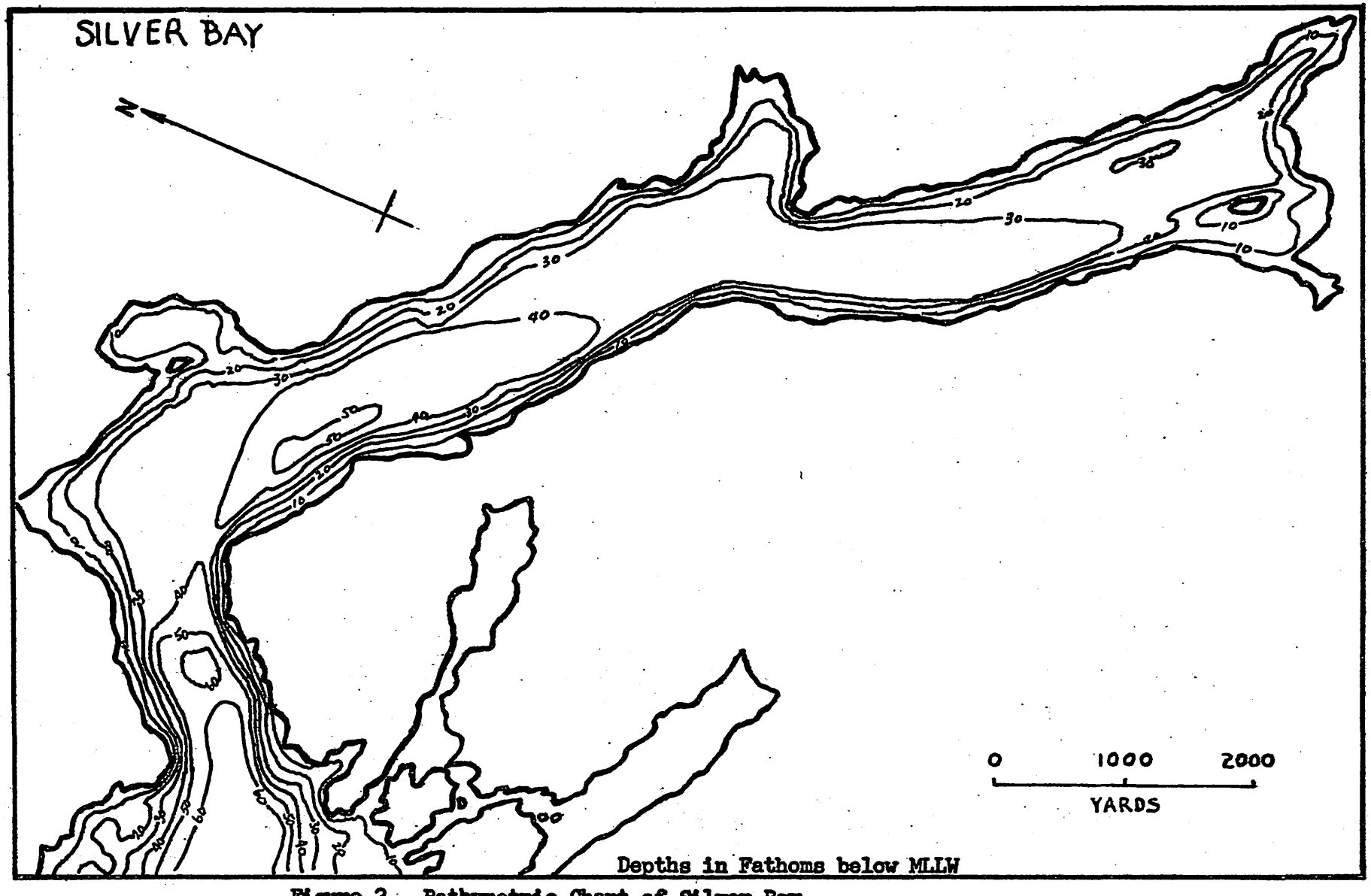

Figure 2. Bathymetric Chart of Silver Bay

relatively fresh water moves seaward toward the mouth of the bay, and overrides an inflow of more saline water moving at velocities much less than those in the surface layer.

The summer observations indicate the layer of outflowing surface water to have a depth of about 15 feet, and a salinity range from nearly zero off the inflowing rivers to 28 °/oo at the mouth of the inlet. In summer most of the inflowing water enters the bay in a layer between depths of 15 feet and 100 feet. "Jet" effects were noticed in the surface layer immediately adjacent to the streams entering the bay. Particularly prominent was the tongue of fresher water extending from Sawmill Creek.

The winter runoff was only 10 percent of the summer runoff. Both the properties of the water and the circulation system observed in March were quite different from those seen during the summer. As expected, the coastal water had changed to denser, colder water. In the observed circulation, the water at depth in Silver Bay was being replaced by water from Sitka Sound, with an accompanying surface outflow. Observations indicate two layers: (a) an outflowing layer, from the surface to a depth of 90 feet, containing about 2 percent fresh water; (b) an inflowing layer, from 90 feet to the bottom, containing more saline water. No jet or asymmetric features were observed in the winter, and the water in Silver Bay and adjacent coastal water were, in general, more homogeneous than during the preceding summer.

The alkalinity, pH, and the phosphate and oxygen values of the waters of Silver Bay and approaches were not unusual for coastal Alaskan waters. They have not been used in this study other than to provide

general confirmation of observed and inferred circulations. A schematic diagram, illustrative of the summer regime of circulation, is shown in Figure 3.

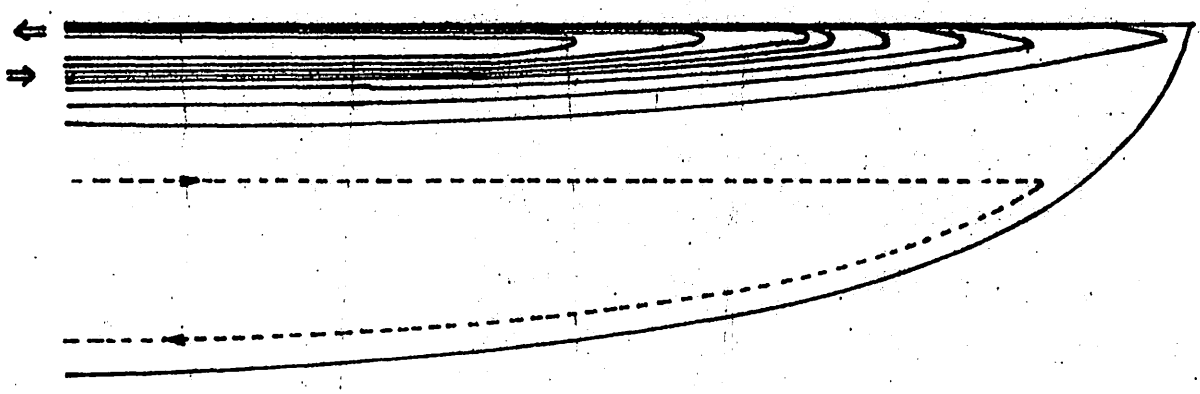

Figure 3. Schematic Illustration of Summer Circulation in Silver Bay

CHAPTER 2

FIELD OBSERVATIONS

2.1 Surveys

A reconnaissance oceanographic survey was made from 16 to 21 May 1956. Two intensive investigations were made later to coincide with periods of maximum and minimum fresh water inflow. The second survey period, from 4 to 11 July 1956, was during the summer conditions of high runoff, relatively high surface temperatures, and low local salinities. The third survey was made from 24 to 30 March 1957, at the local extreme winter oceanographic conditions of minimum runoff, low surface temperatures, and high salinities. Additional data were gathered in Silver Bay from July 1956 to March 1957, by the Alaska Water Pollution Control Board.

Five vessels in all were used during the periods of the surveys. The May survey was completed by the MV BROWN BEAR, research vessel of the Department of Oceanography, University of Washington. In July, the MV BROWN BEAR was joined by the MV SKIPJACK from the United States Fish and Wildlife Service, the MV RANGER VII from the United States Forest Service, and a chartered vessel, the MV ROMANY III. In March, the MV BROWN BEAR was again joined by the MV RANGER VII, and by the MV TEAL from the United States Fish and Wildlife Service. As many as six outboard boats were in regular use in both March and July. The field observations from the three surveys, together with certain additional data gathered by the Alaska Water Pollution Control Board, are reported in

Special Report No. 24 of the Department of Oceanography, University of Washington (Barnes et al. 1956).

2.2 Water Properties

All routine hydrographic stations were taken from the MV BROWN BEAR. Salinity, temperature, oxygen, and phosphate samples were obtained at each station, except that no phosphate samples were obtained at Stations 143-3, 163-24, and 163-26. In addition, pH, alkalinity, BOD, lignin, and Tyndall readings were taken at selected stations.

The same general procedure was followed in each survey period. A series of stations was taken longitudinally along the inlet upon arrival at Silver Bay, and the same stations were reoccupied just prior to departure. Thus, the rates at which water properties within Silver Bay were changing with time may be determined. During most of the remaining time of each survey period, the MV BROWN BEAR occupied an anchor station near the mouth of the bay, during which period a stationary time-series of observations of water properties was made.

Observations were made with an STD (Salinity-temperature-depth recorder), lowering the sensing head vertically at selected positions and towing it just under the surface between these positions. These observations were used to supplement the data from the hydrographic stations. STD observations in July were made from the MV BROWN BEAR; observations in March were made from the MV TEAL.

The positions of the hydrographic, STD, and current stations occupied in Silver Bay and immediate approaches are shown for the May

(Figure 4), July (Figure 5), and March (Figure 6) surveys. The stations occupied by the Alaska Water Pollution Control Board are shown in Figure 7.

Rather large annual variations of temperature and salinity occur in Silver Bay because of the annual fluctuations in meteorological and climatological conditions, as well as because of changes occuring in the off-lying coastal waters. Estimates of the pertinence and relevance of these effects upon the circulation in Silver Bay and upon the general problem of estuarine circulation are noted as they occur. Mean values of salinity and temperature at selected locations along channel just inside the entrance to Silver Bay, (refer to Figure 8) are reported in Table 1.

2.3 Current Measurements at Anchor Stations

The May cruise was primarily reconnaissance. Measurements of temperature, salinity, and currents, while useful for comparison, proved inadequate to accurately evaluate the terms in the equations of motion.

Current measurements were obtained 20 May 1956, at Anchor Station 142-48 for a 24-hour period. All measurements were made from the MV BROWN BEAR with Ekman type current meters. This station was in a shoal area and too close to the mouth of Sawmill Creek to give a representative picture of the currents in Silver Bay. No further analysis is made of the May current measurements in this paper.

Current measurements in July were obtained for a 36-hour period from 0200, 8 July to 1400, 9 July 1957, at three stations across the entrance to Silver Bay. Readings were taken at the surface and at depths of 5, 10, 20, 30, 50 and 100 feet. Additional readings were taken from the MV BROWN BEAR at the center-channel station (Station B) at 20, 40, 60, 75

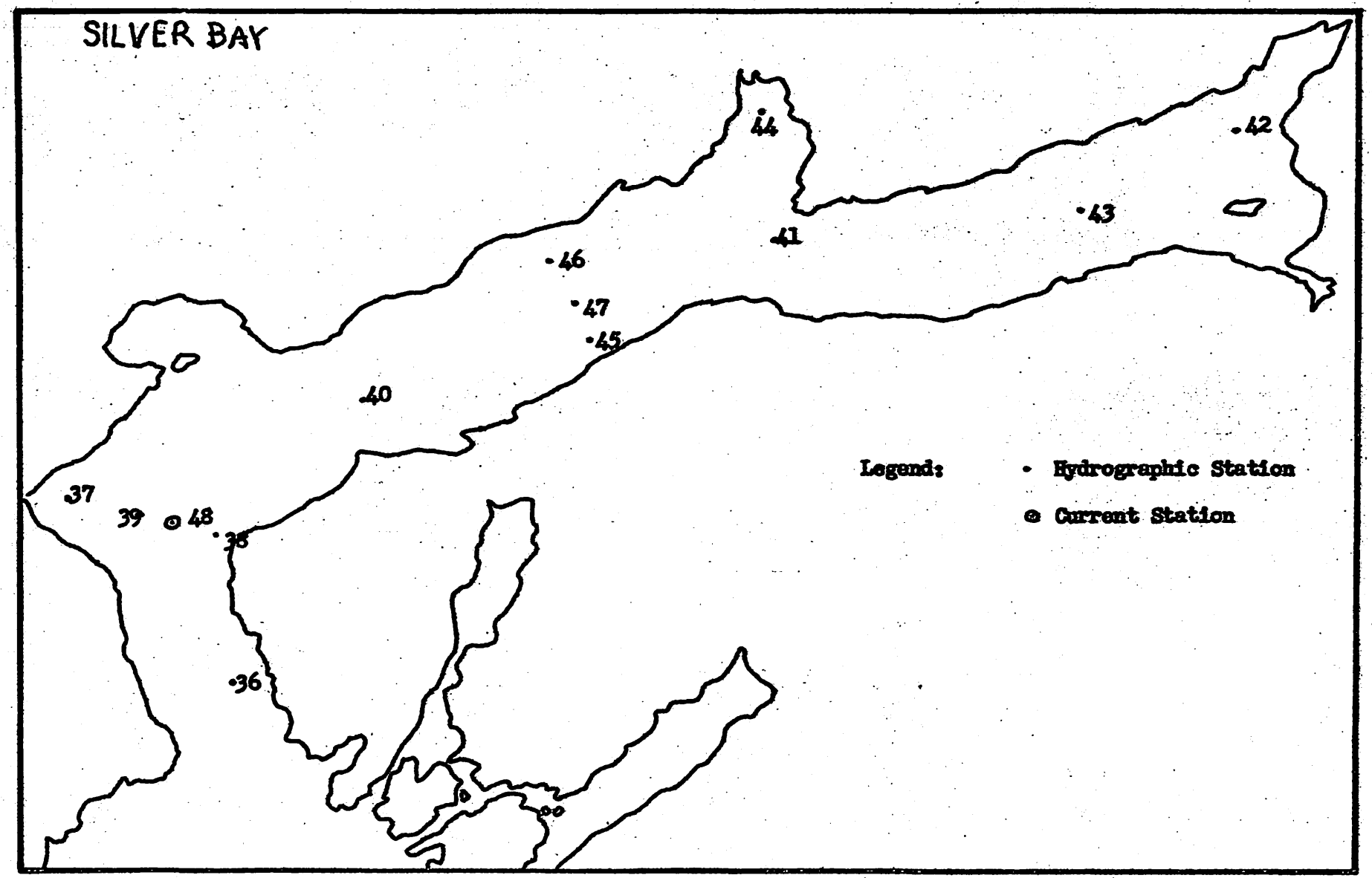

Figure 4. Location of Hydrographic and Current Stations during Cruise 142, May, 1956

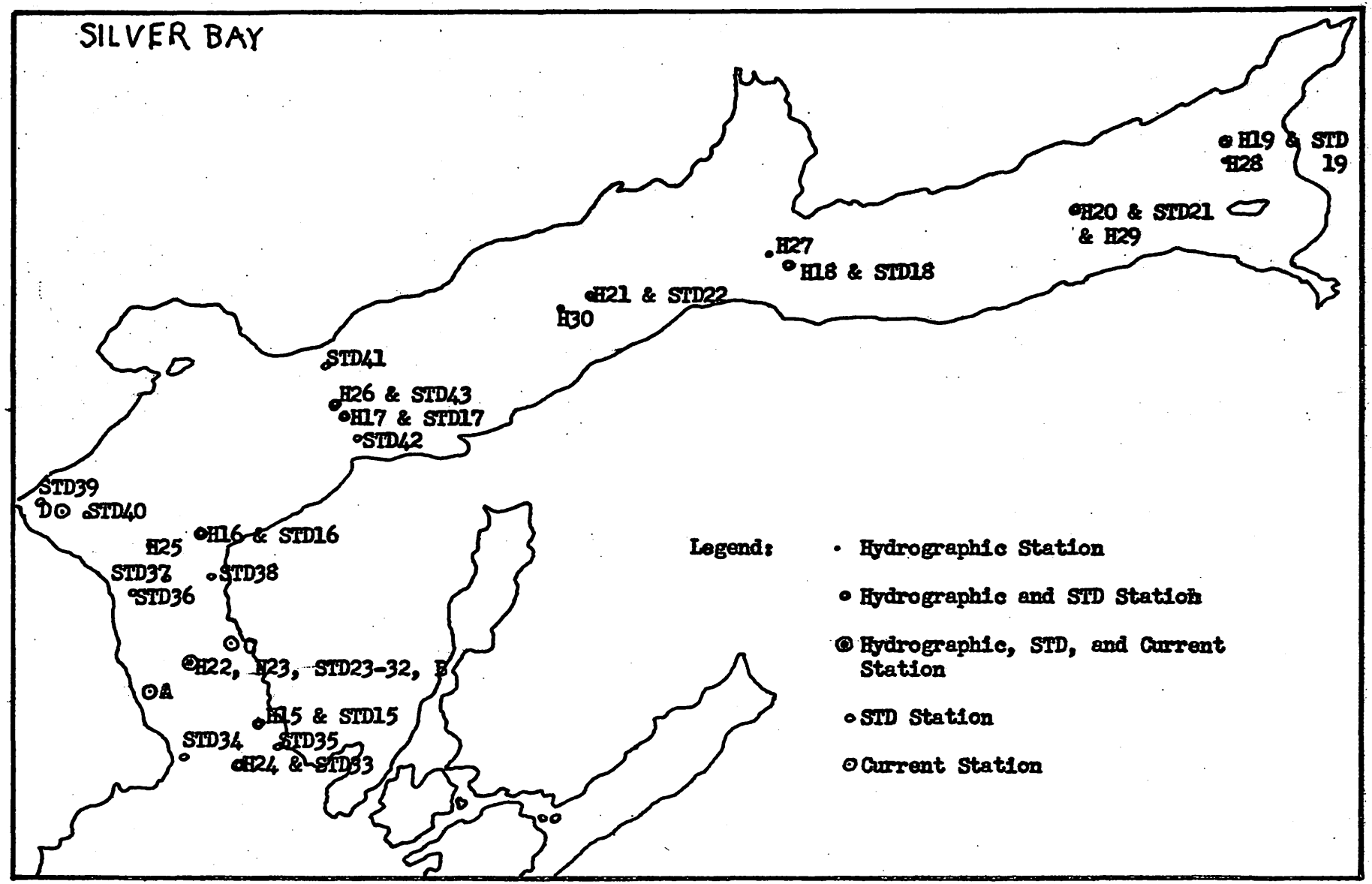

Figure 5. Location of Hydrographic, STD, and Current Stations during Cruise 143, July, 1956

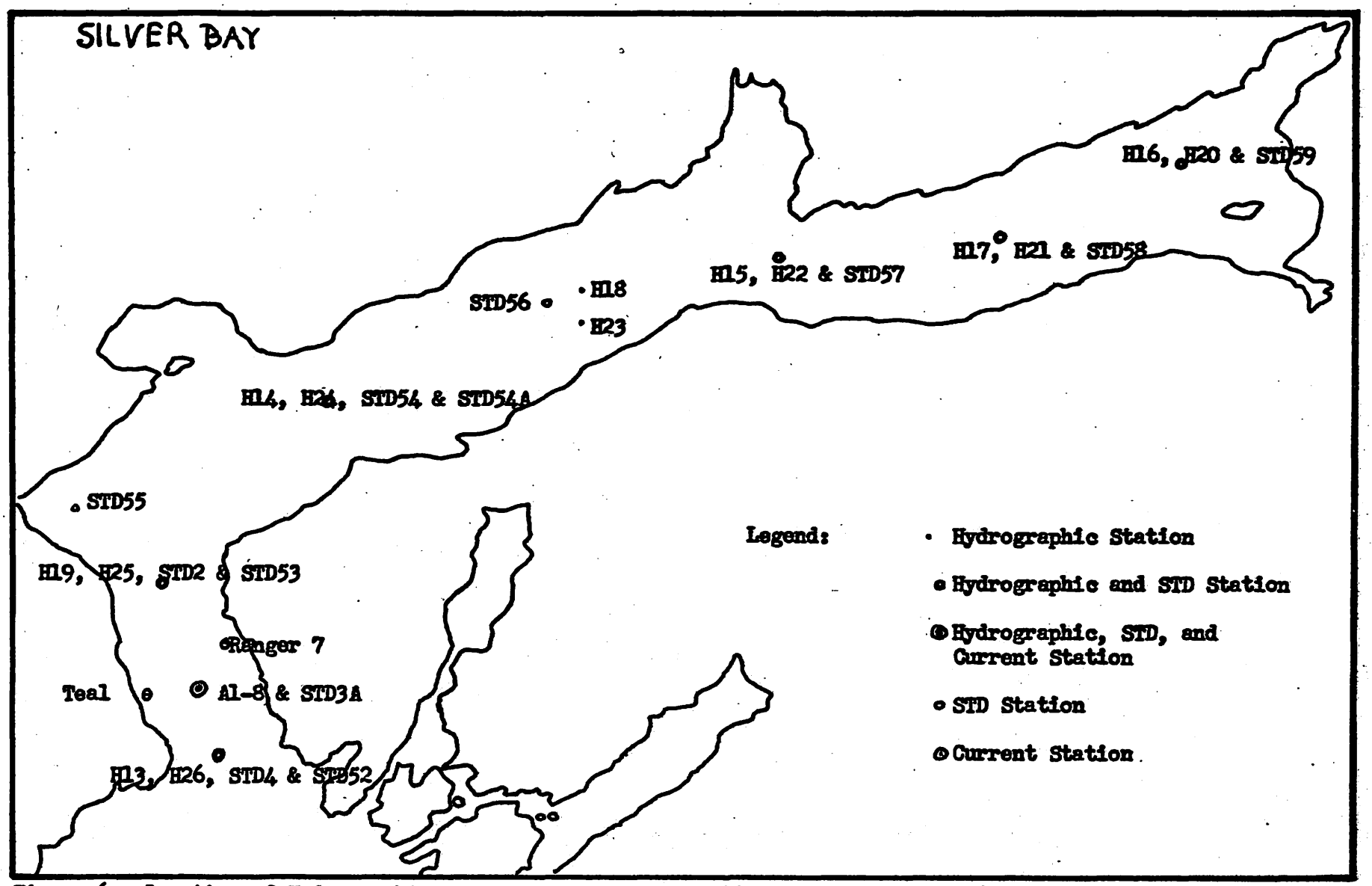

Figure 6. Location of Hydrographic, S-T-D, and Current Stations during Cruise 163, March, 1957

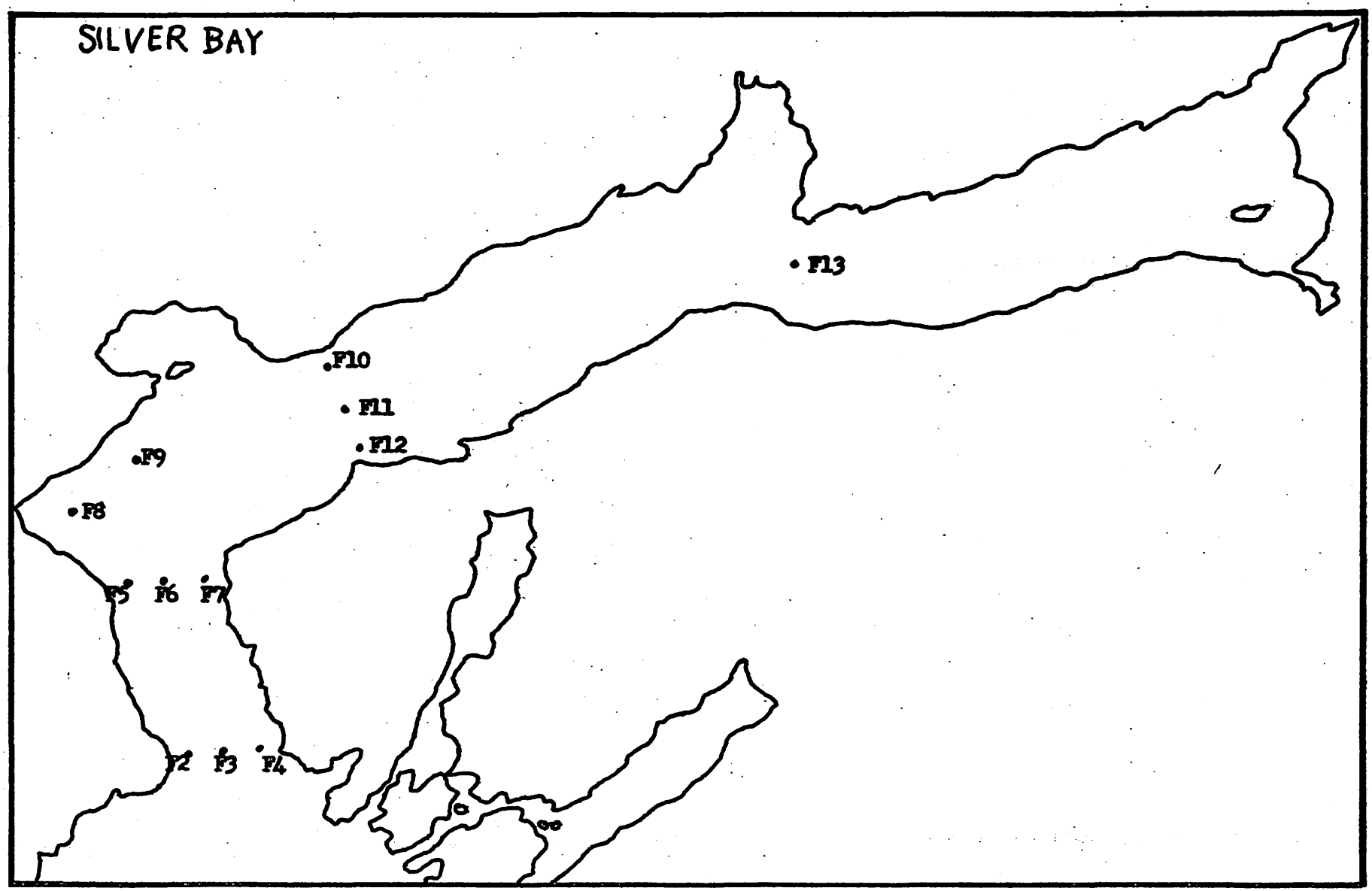

Figure 7. Location of Hydrographic Stations occupied by Alaska Water Pollution Control Board

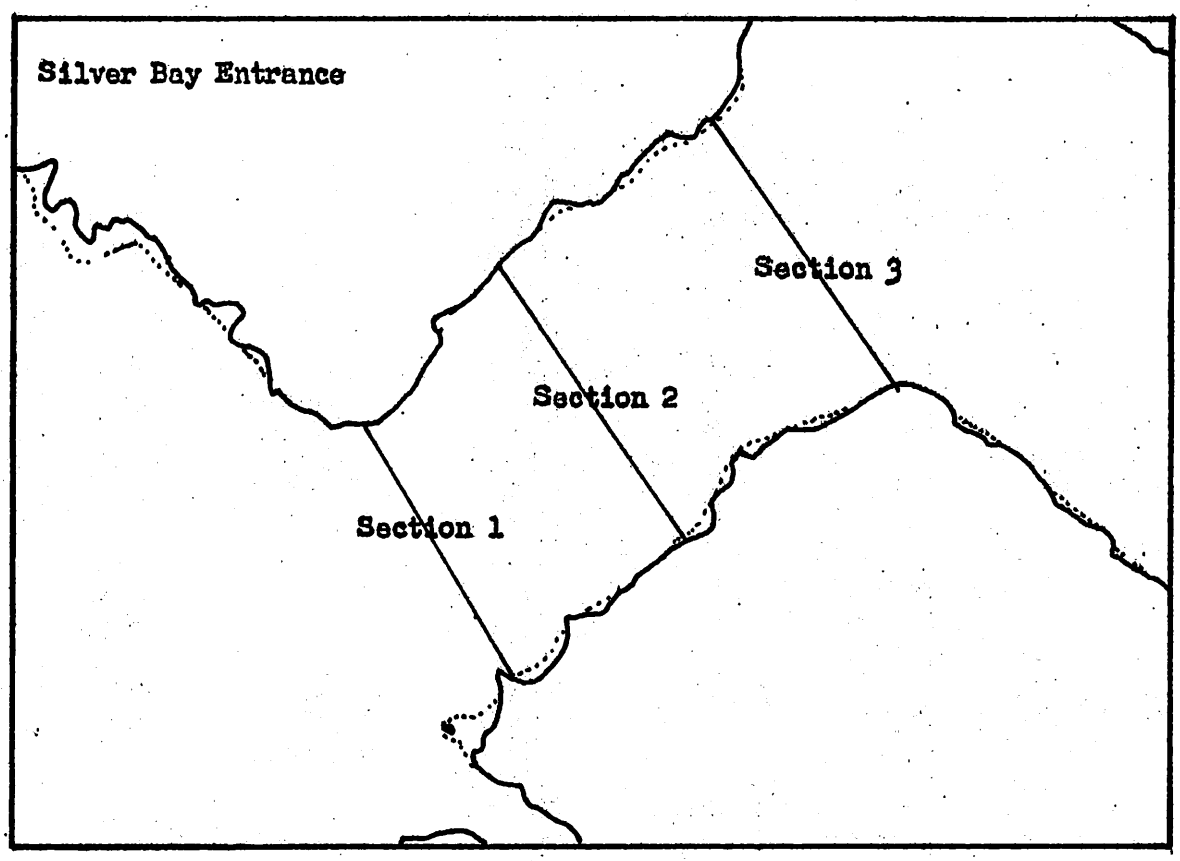

Figure 8. Section Lines at Entrance of Silver Bay

TABLE 1 (A and B)

A. Mean Salinities and Temperatures, 6 to 10 July 1956

Depth	Section 1		Section 2		Section 3	
	Salinity	Temperature	Salinity	Temperature	Salinity	Temperature
m	°/oo	°C	°/oo	°C	°/oo	°C
0	22.8	11.8	20.8	11.65	16.8	11.0
2	30.15	11.7	30.02	11.68	29.89	11.6
4	30.68	11.16	30.66	11.10	30.63	11.02
6	30.79	11.02	30.76	10.87	30.73	10.72
10	31.30	10.48	31.29	10.40	31.28	10.32
20	31.72	8.86	31.71	8.85	31.71	8.84
30	31.77	7.40	31.76	7.35	31.75	7.30
40	31.87	6.80	31.86	6.75	31.85	6.70
50	31.92	6.30	31.91	6.24	31.90	6.20
75	32.01	5.05	32.01	5.03	60m 31.92	-
100	32.07	4.70	32.07	4.65	-	-

B. Mean Salinities and Temperatures, 26 to 30 March 1957

Depth	Section 1		Section 2		Section 3	
	Salinity	Temperature	Salinity	Temperature	Salinity	Temperature
m	°/oo	°C	°/oo	°C	°/oo	°C
0	30.11	-	29.91	4.80	29.70	-
1	31.30	-	31.28	4.90	31.25	-
2	31.50	4.8	31.49	4.82	31.48	4.8
4	31.92	4.7	31.93	4.74	31.93	4.7
7	32.00	4.74	32.01	4.76	32.03	4.78
10	32.03	4.79	32.04	4.80	32.05	4.81
20	32.11	4.80	32.11	4.81	32.11	4.82
30	32.13	4.78	32.13	4.78	32.13	4.79
40	32.15	-	-	-	32.14	-
50	32.16	4.75	32.16	4.75	32.15	4.75
75	32.19	4.76	32.19	4.76	-	-
100	32.21	4.75	32.21	4.75	-	-

and 100 meters. All readings at MV SKIPJACK (Station C) were made by biplane; those at MV RANGER VII (Station A) by biplane and Ekman meter; those at the MV BROWN BEAR by biplane, and by Ekman and Magnesyn meters. The MV RANGER VII also measured currents for a 20-hour period on 8 and 9 July at Station D off the mouth of Sawmill Creek. Measurements were made by biplane and by Ekman meter. These measurements showed relatively high velocities at the surface in the river discharge plume, but little movement of the deeper water. Station D is in the same general area as Station 142-48, occupied in May.

Current measurements in March were obtained for a 60-hour period from 2000, 26 March 1957 to 0800, 29 March, at three stations in approximately the same locations as the stations of the preceding summer. All readings at MV RANGER VII (Station C') were made by biplane and by Ekman meter; those at MV TEAL (Station A') by biplane and by Ekman meter; those at MV BROWN BEAR (Station B') by biplane, and by Ekman and Magnesyn meters. The March and July current measurements are reported in Table 2.

Some difficulty was experienced in determining the direction of deep currents where no direction was determined from the meter because both magnitude and direction were weak and variable. In general, it was assumed that the Ekman and Magnesyn meter readings were more reliable and accurate than the biplane readings and, when doubt occurred, it was resolved in favor of the meter readings. When no direction was obtained from the meter, the direction was assumed to be that of a corresponding biplane reading when such a reading existed.

The same analysis of data was applied to the March and July measurements. Hourly averages of along-channel components were plotted

TABLE 2

Mean Currents at Anchor Station, July 1956 and March 1957.

Depth m	Mean Velocity, July ms^{-1} (negative values indicate inflow)	Mean Velocity, March ms^{-1}
0.5	0.16	0.11
1.5	0.11	-
2	-	0.06
3	0.05	-
5	-	0.015
6	-0.005	-
10	-0.05	0.018
15	-0.03	-
20	-	0.020
30	0.00	0.00
40	-	-0.016
75	-	-0.016
100	-	0.00

for each depth at each station. Velocities were then averaged for each tidal stage. Net and tidal velocities with depth were then computed. Tidal velocities were considered as the mean velocity less the net velocity during a tidal stage. Since it was felt that the center-station current measurements were the most representative of the mean current in the channel, the center measurements were doubly weighted in averaging for the mean currents. The complete analysis is presented in Special Report No. 24 of the Department of Oceanography, University of Washington (Barnes et al. 1956). Current profiles of net current with depth are shown in Figures 9 and 10.

2.4 Drift Sticks and Drift Poles

A series of drift-pole and drift-stick measurements were conducted on 6, 7 and 8 July 1956, and again on 25 through 29 March 1957. The drift-sticks used were 1.5 feet long, and extended approximately one foot

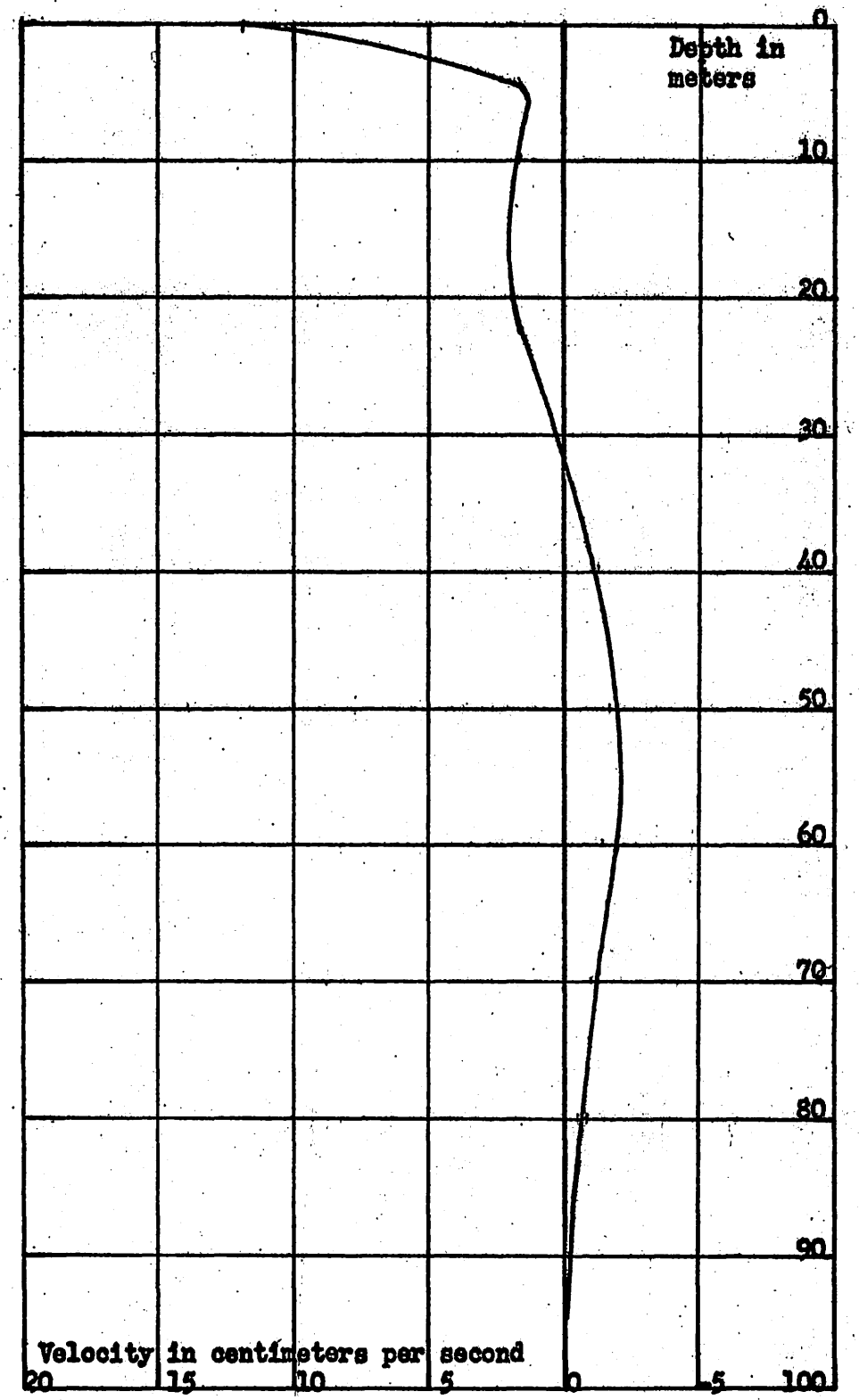

Figure 9. Current Profile with Depth, March, 1957

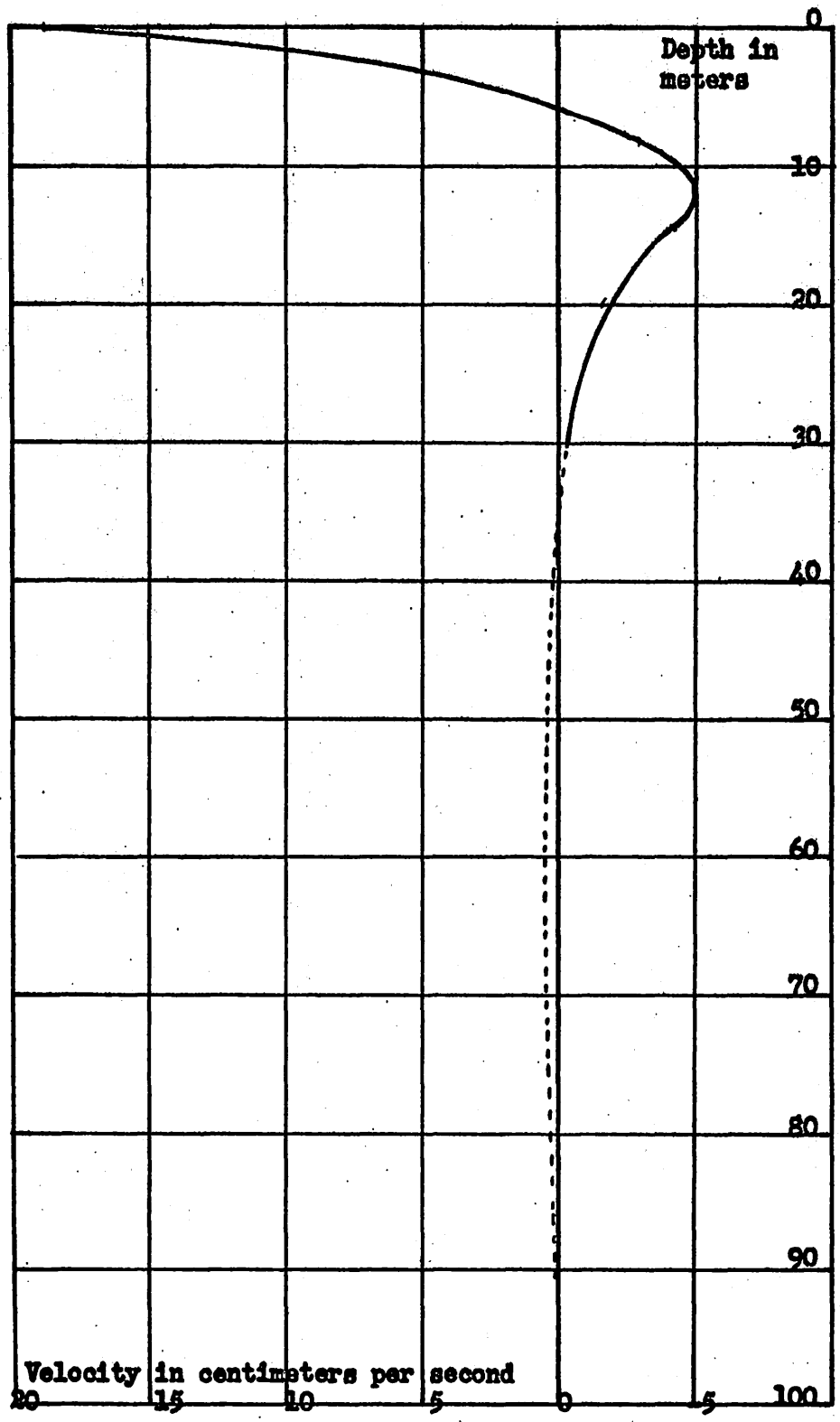

Figure 10. Current Profile with Depth, July, 1956

into the water. The drift-poles used were sixteen feet long, and extended approximately fifteen feet into the water. The results of the observations, where applicable to the present study, are discussed in the paragraph on the inertial accelerations occurring in the surface layer of Silver Bay.

2.5 Dye Studies

Dye streaks were laid across the mouth of Silver Bay and at various points in the inlet during 7 July 1956. The dye streaks were photographed at intervals from an airplane. The dye patterns diffused rapidly and, considering the lack of precise position control and rather long time-intervals between consecutive photographs of a given dye streak, no reliable computations could be based upon the movement of these streaks. In general, however, the dye streaks corroborated the evidence on the surface circulation obtained by other means.

2.6 River Runoff

River runoff in Silver Bay varies from less than 100 cfs to more than 3000 cfs. Approximately half of the fresh water inflow enters through Sawmill Creek. The other major source is the Vodopad River. A small stream at the southwest head of Silver Bay, and a stream in Bear Cove complete the principal fresh water addition. The relation of runoff between Sawmill Creek and the Vadopad River may be estimated by records of the gaged discharges. Discharge from other areas was estimated on the assumption that runoff is directly proportional to the area of the drainage basin. Accepted values for the total estimated fresh water

discharge into Silver Bay are 1720 cfs for the period 4 to 11 July 1956, and 150 cfs for the period 27 to 31 March 1957.

2.7 Biological and Geological Sampling

Extensive biological sampling was undertaken in Silver Bay. Plankton samples, midwater trawls, bottom fauna samples, and beach or shore samples were obtained. Both dredged material and cores were obtained for geological analysis. A complete discussion of the biological and geological analyses may be obtained by referring to Special Report No. 24, Department of Oceanography, University of Washington (Barnes et al. 1956).

2.8 Meteorological Data

Hourly wind observations were made from the MV BROWN BEAR, and data were obtained from the U. S. Weather Bureau for hourly winds at the Sitka Airport (Japonski Island) during the periods of the survey. Annual records of wind, temperature, and precipitation at Sitka were obtained from the U. S. Coast Pilot, Southeast Alaska. These records and the hourly winds are listed in Special Report No. 24, Department of Oceanography, University of Washington (Barnes et al. 1956). Mean values of the wind for 6-hour intervals as recorded at the MV BROWN BEAR are listed in Table 3.

TABLE 3

Mean Wind Speed as Recorded at MV BROWN BEAR

(Values given are for mean wind for 6-hour interval preceding listed time.)

Location	Date	Time hr	Dir. °T	Vel. knots
	1956			
N. End Silver Bay	6 July	0600	--	0
"		1200	--	0
Entrance of Silver Bay		1800	245	2
Eastern Channel	7 July	0000	265	8
N. End Silver Bay		0600	120	2
Entrance of Silver Bay		1200	050	4
N. End Silver Bay		1800	110	2
NW of Sugarloaf (Anchor Station)	8 July	0000	060	6
"		0600	050	4
"		1200	045	5
"		1800	v.	4
"	9 July	0000	010	1
"		0600	035	3
"		1200	210	8
"		1800	nr	nr
Entrance Channel	10 July	0000	v.	1
S. End Silver Bay		0600	--	0
	1957			
S. End Silver Bay	25 March	0600	130	2
N. End Silver Bay		1200	110	4
"		1800	--	0
Entrance of Silver Bay	26 March	0000	--	0
"		0600	045	7
E. of Sugarloaf		1200	050	2
NW of Sugarloaf (Anchor Station)		1800	nr	nr
"	27 March	0000	040	4
"		0600	055	3
"		1200	070	5
"		1800	045	6
"	28 March	0000	035	5
"		0600	030	4
"		1200	v.	4
"		1800	--	0
"	29 March	0000	v.	3
"		0600	030	2
"		1200	055	2
S. End Silver Bay		1800	120	9
Eastern Channel	30 March	0000	080	9

v. Variable
nr Not Recorded

CHAPTER 3

THE DIFFERENTIAL EQUATIONS OF MOTION

3.1 Introduction

The basic method of this study is to obtain the equations of motion for the circulation of the water in an estuary in such a form that the value of all the terms may be either computed directly from measurement or inferred. Assume that a quasi-steady state exists within the estuary, and take the time mean of equations. For the coordinate system, let the x-axis point seaward along the inlet, let the y-axis point laterally toward the shore on the right, and let the z-axis point downward vertically from a level surface just beneath the upper boundary. The coordinate system is illustrated in Figure 11.

3.2 The Longitudinal Component of the Equations of Motion

With the coordinate system just described, the x-component of the equation of motion may be written for instantaneous values of the various parameters:

$$\frac{\partial v_x}{\partial t} + v_x \frac{\partial v_x}{\partial x} + v_y \frac{\partial v_x}{\partial y} + v_z \frac{\partial v_x}{\partial z} = -\frac{1}{\rho}\frac{\partial p}{\partial x} + f v_y + \frac{1}{\rho}\left(\frac{\partial F_{xx}}{\partial x} + \frac{\partial F_{xy}}{\partial y} + \frac{\partial F_{xz}}{\partial z}\right) + X \qquad (1)$$

v_x, v_y, v_z represent the instantaneous velocities in the x, y, and z directions, respectively
f represents the Coriolis parameter, $2\omega \sin \varphi$
ρ represents the density of water
p represents the pressure
X represents body forces in the x-direction
F_{ij} represents the appropriate components of the molecular stress related to the motion.

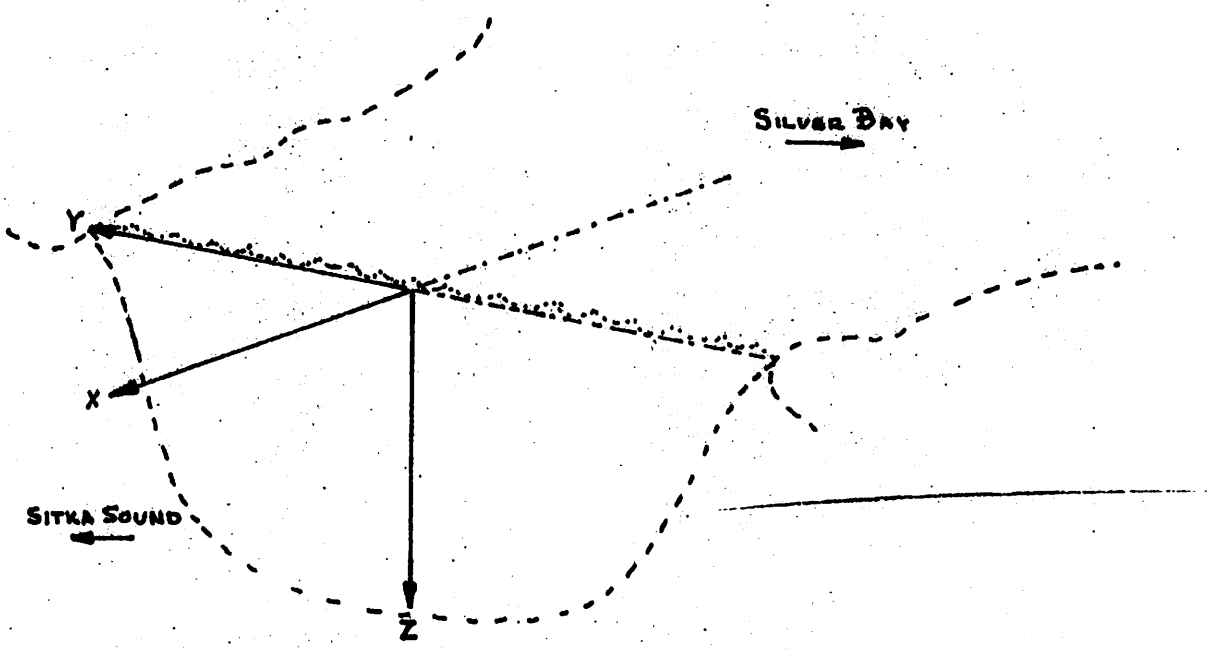

Figure 11. Coordinate System as Applied at Mouth of Silver Bay

The time mean of Equation (1) is now taken after substituting for the instantaneous velocity, v_i, a sum of a mean velocity and a velocity deviation from the mean velocity. To facilitate comparison, we shall follow the method used by Pritchard (1956) in evaluating the equations of motion for Chesapeake Bay, and consider the instantaneous velocity to consist of three terms:

(a) a time mean velocity, $\bar{v}_i$, obtained by averaging over one or more tidal cycles (this mean velocity has components along the longitudinal (x) and vertical (z) axes, but the lateral component is assumed negligible, that is $\bar{v}_y = 0$);

(b) an oscillatory tidal velocity, U, which is directed up and down the longitudinal axis of the estuary (this term is assumed to be a function of x only, and to vary according to the simple harmonic function $U = U_o \cos \phi$, where both the phase of current, ($\cos \phi$) and the tidal velocity amplitude (U_o) may be functions of distance along the channel);

(c) a velocity deviation, v_i', which results from those turbulent fluctuations which have a time scale smaller than the period employed in the averaging process (the period of averaging used here is two tidal cycles).

The three components of the instantaneous velocity thus become:

$$v_x = \bar{v}_x + v_x' + U$$

$$v_y = v_y'$$

$$v_z = \bar{v}_z + v_z'$$

These velocity terms are now introduced into Equation (1), and the time mean of Equation (1) taken over one or more tidal cycles. There is no reason to suppose any relation between v_x', v_y', v_z' on the one hand and the tidal component U on the other. Thus, terms of the type $\langle v_x' U \rangle$ will not appear in the mean equation. We further assume that the molecular stress terms are small in comparison with the so-called eddy stress terms, and the molecular stresses may be considered as included in the eddy terms. Under these conditions, the time mean of Equation (1) for mean steady state is:

$$\bar{v}_x \frac{\partial \bar{v}_x}{\partial x} + \bar{v}_z \frac{\partial \bar{v}_x}{\partial z} + U_o \frac{\partial U_o}{\partial x} =$$

$$-\left\langle \frac{1}{\rho} \frac{\partial p}{\partial x} \right\rangle - \frac{\partial}{\partial x}\langle v_x' v_x' \rangle - \frac{\partial}{\partial z}\langle v_x' v_z' \rangle - \frac{\partial}{\partial y}\langle v_x' v_y' \rangle + f\bar{v}_y + X \qquad (2)$$

Several simplifying assumptions may be made before evaluating Equation (2) for Silver Bay:

(a) The value of U_o is determined from the volume of intertidal water entering Silver Bay. The value for U_o is found to be 1.9 cm s^{-1} at the anchor station, Section 2. The small values occur because of the large depth of Silver Bay (350 feet), as compared to the mean tidal range (7 feet). Not only is the velocity itself small, but the change in velocity along the channel is small as the decrease in cross-sectional area of the channel approximately compensates for the change in intertidal volume proceeding along the channel. The value of the term, $U_o \frac{\partial U_o}{\partial x}$, appearing in Equation (2) may now be computed,

and is found to be 4×10^{-6} cm s^{-2}. Since no significance is attached to values of less than 1×10^{-5} occurring in the other terms of Equation (2), $U_o \frac{\partial \bar{U}}{\partial x}$ may be neglected in Silver Bay. It may be noted here that in an investigation of a coastal plain estuary, the James River estuary (Pritchard, 1954) the value of $U_o \frac{\partial U_o}{\partial x}$ was found to be approximately sixty times the value found in Silver Bay and represented an important contribution to the equation of mean steady state longitudinal motion.

(b) In the study of the salt balance for Silver Bay, Paragraph 5.2, the horizontal component of the turbulent flux of salt is shown to be negligible compared to the horizontal advection of salt. If we assume by analogy that the horizontal component of the turbulent flux of momentum is also negligible compared to the other terms in the equation of motion, then the terms:

$$\frac{\partial}{\partial x}\langle v_x' v_x' \rangle, \quad \frac{\partial}{\partial x}\langle v_x' v_y' \rangle, \quad \frac{\partial}{\partial y}\langle v_x' v_z' \rangle \text{ and } \quad \frac{\partial}{\partial y}\langle v_x' v_y' \rangle$$

will drop from the equations in which they may appear.

(c) Since the value of $\bar{v}_y$ is assumed to be zero, the term involving the Coriolis parameter will not appear in the equation of the mean motion.

(d) No body forces affecting the longitudinal equation have been observed, and $X = 0$. Under the conditions and assumptions stated above, Equation (2) becomes:

$$v_x \frac{\partial v_x}{\partial x} + v_z \frac{\partial v_x}{\partial z} = -\left\langle \frac{1}{\rho} \frac{\partial p}{\partial x} \right\rangle - \frac{\partial}{\partial z}\langle v_x' v_z' \rangle \qquad (3)$$

Equation (3) has been evaluated in Silver Bay under conditions of flow existing in summer and in winter. The values obtained are representative of Section 2, approximately 0.5 km. inland from the mouth of the estuary. Values for Equation (3) are reported in Tables 4 and 5.

TABLE 4

Comparison of Terms in the Equation of Motion - July*

z m	$\frac{1}{\rho}\frac{\partial \bar{p}}{\partial x}$	$\bar{v}_x \frac{\partial \bar{v}_x}{\partial x}$	$\bar{v}_z \frac{\partial \bar{v}_x}{\partial z}$	$\frac{\partial}{\partial z}\langle v_x' v_z' \rangle$
0	-440	150	0	290
1	-175	90	35	50
2	- 20	37	52	- 69
3	- 10	17	45	- 52
4	- 6	4	34	- 32
5	- 5	0	27	- 22
6	- 3	0	22	- 19
7	- 2	2	19	- 17
8	- 1	4	15	- 18
9	- 0.5	7	9	- 15
10	- 0.5	11	0	- 11
15	- 0.5	5	- 1	- 4
20	- 0.5	2	0	- 2
25	- 0.5	1	0	- 1
30	- 0.5	0	0	0.5
35	- 0.5	0	0	0.5
40	- 0.5	0	0	0.5
45	- 0.5	0	0	0.5
50	- 0.5	0	0	0.5
55	- 0.5	0	0	0.5
60	- 0.5	0	0	0.5
65	- 0.5	0	0	0.5
70	- 0.5	0	0	0.5
75	- 0.5	0	0	0.5
80	- 0.5	0	0	0.5
85	- 0.5	0	0	0.5
90	- 0.5	0	0	0.5
95	- 0.5	0	0	0.5
100	- 0.5	0	0	0.5

*All units are cm sec^{-2} x 10^5

TABLE 5

Comparison of Terms in the Equation of Motion - March*

z m	$\frac{1}{\rho}\frac{\partial \bar{p}}{\partial x}$	$\bar{v}_x \frac{\partial \bar{v}_x}{\partial x}$	$\bar{v}_z \frac{\partial \bar{v}_x}{\partial z}$	$\frac{\partial}{\partial z}\langle v_x' v_z' \rangle$
0	-20	18	0	2
1	- 5	9	3	- 7
2	0	4	5	- 9
3	2	1	4	- 7
4	4	0	4	- 8
5	4	0	2	- 6
6	3	0	0	- 3
7	2	0	0	- 2
8	1	0		- 1
9	0	0		0
10	- 1	0		1
15	- 3	0		3
20	- 4	0		4
25	- 4	0		4
30	- 3	0		3
35	- 2	0		2
40	0	0		0
45	2	0		- 2
50	3	0		- 3
55	4	- 1		- 3
60	5	- 1		- 4
65	5	- 1		- 4
70	4	- 2		- 2
75	3	- 1		- 2
80	2	0		- 2
85	1	0		- 1
90	- 1	0		1
95	- 3	0		3
100	- 5	0		5

*All units are cm sec^{-2} x 10^5

3.3 The Lateral and Vertical Components of the Equation of Motion

By means similar to those used in the derivation of Equation (3), equations may be obtained for the lateral and vertical components of the equations of motion. The same assumptions are used except that body forces,

such as centrifugal forces, must now be considered. In terms of an eddy coefficient: $\langle v_y' v_z' \rangle = - \rho N_z \frac{\partial v_y}{\partial z}$. Since we have assumed $\bar{v}_y = 0$, then $\langle v_y' v_z' \rangle = 0$. Due to curvature of the channel, the effects of centrifugal force must also be considered. Let Y represent the component of such forces in the y-direction. Then the lateral equation for mean steady state becomes:

$$\left\langle \frac{1}{\rho} \frac{\partial p}{\partial y} \right\rangle = f \bar{v}_x - Y \tag{4}$$

Insufficient data exist for accurate determination of Equation (4) from the available summer observations. The equation was investigated for March conditions on the basis of the available observations, and the results are discussed in Chapter IV.

Similarly the vertical equation for mean steady state becomes:

$$\bar{v}_x \frac{\partial \bar{v}_z}{\partial x} + \bar{v}_z \frac{\partial \bar{v}_z}{\partial z} = - \left\langle \frac{1}{\rho} \frac{\partial p}{\partial z} \right\rangle + g \tag{5}$$

Under conditions existing within Silver Bay, the inertial terms in Equation (5) are negligible in comparison with the pressure and the gravitational terms, and the hydrostatic equation, Equation (6), will be valid.

$$0 = - \frac{1}{\rho} \frac{\partial \bar{p}}{\partial z} + g \tag{6}$$

CHAPTER 4

EVALUATION OF TERMS IN THE EQUATIONS OF MEAN MOTION

4.1 Procedure

The various terms in Equations (3) and (4) have been evaluated from the data obtained in the Silver Bay surveys. In general, sufficient data are available to evaluate the various inertial and pressure terms. Values for the stress terms are derived essentially as solutions of the equations. Since the equations each involve only one unknown stress term, the equation may be solved for the stress in terms of the known and measured quantities. Evaluations have been made for both summer and winter conditions. Since the method of evaluating each term has not been the same at each season, nor necessarily the same at all depths at any given time, the evaluation for each term is treated separately.

4.2 Evaluation of $\left\langle \frac{1}{\rho} \frac{\partial p}{\partial x} \right\rangle$ in July

$\left\langle \frac{1}{\rho} \frac{\partial p}{\partial x} \right\rangle$ was evaluated as $\frac{1}{\rho} \frac{\partial \bar{p}}{\partial x}$. Equation (6) is first integrated:

$$p = g \int_{-\rho}^{z} \rho dz \qquad (7)$$

The resulting Equation (7) is then differentiated with respect to the x-coordinate:

$$\frac{\partial p}{\partial x} = -g\rho_s \frac{d\zeta}{dx} + g \int_{0}^{z} \frac{\partial \rho}{\partial x} dz \qquad (8)$$

The term, $\frac{d\zeta}{dx}$ representing the surface slope, in Equation (8) may be evaluated if the value of the stress is known at two points on the vertical profile. Equation (3) is rewritten using Equation (8) and the notation $\langle v_x' v_z' \rangle = F_z$

$$\frac{\partial F_z}{\partial z} + \frac{d\zeta}{dx} + g\int_0^z \frac{\partial \rho}{\partial x}\, dz = -\rho\left(\bar{v}_x \frac{\partial \bar{v}_x}{\partial x} + \bar{v}_z \frac{\partial \bar{v}_x}{\partial z}\right) \tag{9}$$

Equation (9) is now integrated between z' and z'', the two depths where the value of the stress is known:

$$F_{z''} - F_{z'} + g\rho_s \frac{d\zeta}{dx}(z'' - z') + g\int_{z'}^{z''}\int_0^z \frac{\partial \rho}{\partial x}\, dz\,dz = -\rho\int_{z'}^{z''}\left(\bar{v}_x \frac{\partial \bar{v}_x}{\partial x} + \bar{v}_z \frac{\partial \bar{v}_x}{\partial z}\right) dz \tag{10}$$

Several methods are available for the determination of the stress at some depth. Wind measurements would enable direct determination of the surface stress. However, sufficient wind data is not available to obtain accurate results. Using the surface stress also requires integrating the relatively poorly known inertial terms, $\left(\bar{v}_x \frac{\partial \bar{v}_x}{\partial x}\right.$ and $\left.\bar{v}_z \frac{\partial \bar{v}_x}{\partial z}\right)$, through the upper layer in order to obtain $\frac{d\zeta}{dx}$. For these reasons, values other than the surface stress were used.

Using the square law for bottom stress, we may assume that the force of friction on the channel bottom is in the direction of the bottom current, and of magnitude:

$$F_b = k\,\rho_b\,u_b^2 \tag{11}$$

Where ρ_b is the density of the bottom water, u_b is the water velocity measured 1 m above the bottom, and for all values of u_b, k will be taken

as 0.0025 (Proudman, 1953). In July, the velocity was zero at 100 m, several meters above the bottom. Thus $F_{100} = 0$.

We may also take advantage of the fact that the term $\langle v_x' v_z' \rangle$ may be regarded as related to $\frac{\partial \bar{v}_x}{\partial z}$ such that $\langle v_x' v_z' \rangle = 0$ when $\frac{\partial \bar{v}_x}{\partial z} = 0$ at a region of symmetry. F_z was taken as zero at 12 m where $\frac{\partial \bar{v}_x}{\partial z} = 0$. This choice would seem to involve less uncertainty than attempting to evaluate the surface stress. Thus, for July:

(a) $\int_0^z \frac{\partial \rho}{\partial x} dz$ is independent of z in range z = 12 to 100 m

(b) $\int_{12}^{100} \left(\bar{v}_x \frac{\partial v_x}{\partial x} + v_z \frac{\partial v_x}{\partial z} \right) dz = 0$ in range z = 12 to 100 m

(c) $F_{12} = F_{100} = 0$

Equation (10) may thus be simplified to:

$$\frac{d\zeta}{dx} = -\frac{1}{\rho_s} \int_0^z \frac{\partial \rho}{\partial x} dz \qquad (12)$$

Using $\rho_s = 1.02$ g cm^{-3}, and $\int_0^{100} \frac{\partial \rho}{\partial x} dz = 120$ g cm^{-3} from Table 4, we obtain $\frac{d\zeta}{dx} = -1.2 \times 10^{-6}$. Equation (8) is then evaluated using the value of the surface slope just obtained from Equation (10). The evaluation is shown in Table 6.

4.3 Evaluation of $\left\langle \frac{1}{\rho} \frac{\partial p}{\partial x} \right\rangle$ for March

The same procedure is followed as in Section 4.2. The difficulty in obtaining accurate mean wind stresses and integrating $\left(\bar{v}_x \frac{\partial \bar{v}_x}{\partial x} + \bar{v}_z \frac{\partial \bar{v}_x}{\partial z} \right)$ through the surface layer again precludes using a wind stress at tne surface. The upper limit was obtained by noticing that the velocity gradient goes to zero at 18 m in a region of approximate symmetry. Thus $F_{18} = 0$. The bottom stress was calculated, and again there was a negligible

TABLE 6

Evaluation of $\frac{1}{\rho}\frac{\partial \bar{p}}{\partial x}$ in July

z (m)	$g\frac{\partial \rho}{\partial x}$ ($gm\ cm^{-3}\ sec^{-2}$ x 10^7)	$g\frac{\partial \rho}{\partial x}\,dz$ ($gm\ cm^{-2}\ sec^{-2}$ x 10^5)	$g\int_0^z \frac{\partial \rho}{\partial x}\,dz$ ($gm\ cm^{-2}\ sec^{-2}$ x 10^5)	$g\rho_s\frac{d\zeta}{dx}$ ($gm\ cm^{-2}\ sec^{-2}$ x 10^5)	$\frac{1}{\rho}\frac{\partial \bar{p}}{\partial x}$ ($cm\ sec^{-2}$ x 10^5)
0	100	50	0	- 120	- 120
1	45	45	50	- 120	- 70
2	14	14	95	- 120	- 25
3	5	5	109	- 120	- 11
4	0	0	114	- 120	- 6
5	1	1	114	- 120	- 6
6	2	3	115	- 120	- 5
8	1	2	118	- 120	- 2
10	0	0	120	- 120	-
			120	- 120	-
		No change to bottom			

velocity at the bottom, giving $F_{100} = 0$. Thus for March:

(a) $\int_{18}^{100}\int_{0}^{z} \frac{\partial \rho}{\partial x}\, dz'dz = 172$ from Table 7

(b) $\int_{18}^{100} \left(v_x \frac{\partial v_x}{\partial x} + v_z \frac{\partial v_x}{\partial z} \right) dz = 0$

(c) $F_{18} = F_{100} = 0$

Equation (10) is then solved to give $\frac{d\zeta}{dx} = -2.1 \times 10^{-7}$. Equation (8) is then evaluated, using this value of $\frac{d\zeta}{dx}$, in Table 7.

4.4 Evaluation of $\bar{v}_x \frac{\partial \bar{v}_x}{\partial x}$ for July

Direct current measurements were made only at the second cross-section, so no direct determination of the longitudinal current variation is possible. Mean values for each layer may, however, be determined from consideration of the salt balance. We assume that the current profile at Section 1 and Section 3 will be similar to the actual profile measured at the intermediate Section 2. We further assume that the depth of no net horizontal motion is reasonably constant throughout this portion of the channel at a depth of 5.15 meters. Although no quantitative measurements are available to support these assumptions, qualitative observation of drift-pole velocities along the bay, and the movement of dye streaks introduced into the water at various depths established the fact that the current profiles are similar throughout the region, with the highest velocities at the surface, dropping to zero at a reasonably constant depth of no net horizontal motion.

Values of $\bar{v}_x \frac{\partial \bar{v}_x}{\partial x}$ are first calculated for the upper, outflowing layer. Here we further assume that salt enters the segment as a result of advective processes only. This must be true between the layers as the

TABLE 7

Evaluation of $\frac{1}{\rho}\frac{\partial \bar{p}}{\partial x}$ for March

z (m)	$g\frac{\partial \rho}{\partial x}$ (gm cm^{-3}sec^{-2} x 10^7)	$g\frac{\partial \rho}{\partial x}\delta z$ (gm cm^{-2}sec^{-2} x 10^5)	$g\int\frac{\partial \rho}{\partial x}dz$ (gm cm^{-2}sec^{-2} x 10^5)	$g\int\frac{\partial \rho}{\partial x}dz\delta z$ (gm cm^{-1}sec^{-2} x 10^2)	$g\iint\frac{\partial \rho}{\partial x}dzdz$ (gm cm^{-1}sec^{-2} x 10^2)	$g\,\rho_s\frac{d\zeta}{dx}$ (gm cm^{-2}sec^{-2} x 10^5)	$\frac{1}{\rho}\frac{\partial \bar{p}}{\partial x}$ (cm sec^{-2} x 10^5)
0	25	15	0			- 20	- 20
			15			- 20	- 5
1	5	5					
			20			- 20	0
2	2	2					
			22			- 20	2
3	2	2					
			24			- 20	4
4	0	0					
			24			- 20	4
5	- 1	- 1					
			23			- 20	3
6	- 1	- 1					
			22			- 20	2
7	- 1	- 1					
			21			- 20	1
8	- 1	- 1					
			20			- 20	0
9	- 1	- 1					
			19			- 20	- 1
10	- 1	- 2					
			17			- 20	- 3

(continued)

TABLE 7 (continued)

z (m)	$g\frac{\partial \rho}{\partial x}$ (gm cm^{-3}sec^{-2} x 10^7)	$g\frac{\partial \rho}{\partial x}\delta z$ (gm cm^{-2}sec^{-2} x 10^5)	$g\int\frac{\partial \rho}{\partial x}dz$ (gm cm^{-2}sec^{-2} x 10^5)	$g\int\frac{\partial \rho}{\partial x}dz\delta z$ (gm cm^{-1}sec^{-2} x 10^2)	$g\iint\frac{\partial \rho}{\partial x}dzdz$ (gm cm^{-1}sec^{-2} x 10^2)	$g\,\rho_s\frac{d\zeta}{dx}$ (gm cm^{-2}sec^{-2} x 10^5)	$\frac{1}{\rho}\frac{\partial \bar{p}}{\partial x}$ (cm sec^{-2} x 10^5)
15	- 0.2	- 1			0		
			16	8		- 20	- 4
20	0	0			8		
			16	8		- 20	- 4
25	0.2	1			16		
			17	8		- 20	- 3
30	0.2	1			24		
			18	9		- 20	- 2
35	0.4	2			33		
			20	10		- 20	0
40	0.4	2			43		
			22	11		- 20	2
15	0.2	1			54		
			23	11		- 20	3
50	0.2	1			65		
			24	12		- 20	4
55	0.2	1			77		
			25	12		- 20	5
60	0	0			89		
			25	12		- 20	5
65	- 0.2	- 1			101		
			24	12		- 20	4
70	- 0.2	- 1			113		
			23	11		- 20	3
75	- 0.2	- 1			124		

(continued)

TABLE 7 (continued)

z (m)	$g\frac{\partial \rho}{\partial x}$ (gm cm^{-3}sec^{-2} x 10^7)	$g\frac{\partial \rho}{\partial x}\delta z$ (gm cm^{-2}sec^{-2} x 10^5)	$g\int\frac{\partial \rho}{\partial x}dz$ (gm cm^{-2}sec^{-2} x 10^5)	$g\int\frac{\partial \rho}{\partial x}dz\delta z$ (gm cm^{-1}sec^{-2} x 10^2)	$g\iint\frac{\partial \rho}{\partial x}dzdz$ (gm cm^{-1}sec^{-2} x 10^2)	$g\rho_s\frac{d\gamma_s}{dx}$ (gm cm^{-2}sec^{-2} x 10^5)	$\frac{1}{\rho}\frac{\partial \bar{p}}{\partial x}$ (cm sec^{-2} x 10^5)
			22	11		- 20	2
80	- 0.2	- 1			135		
			21	10		- 20	1
85	- 0.4	- 2			145		
			19	9		- 20	- 1
90	- 0.4	- 2			154		
			17	8		- 20	- 3
95	- 0.4	- 2			162		
			15	7		- 20	- 5
100					169		

horizontal gradient of salinity is negligibly small in the lower layer. We may then consider the transport across each section as consisting of a constant volume of water of salinity 23.6 °/oo, entering at Section 3, (see Figure 8) and a varying quantity of advected salt water of salinity 31.2 °/oo, from the layer which lies below the depth of no net motion. Mean salinities at the three cross-sections are computed in Table 8 A. One-meter increments are used, and $\bar{v}_{x,z}/\bar{v}_s$ is the ratio of velocity at depth to surface velocity. The ratios are taken to be the same for all three sections, and are the observed values at Section 2. The mean salinity is obtained as:

$$s_m = \frac{\Sigma\, sT\bar{v}}{\Sigma\, T\bar{v}} \tag{13}$$

Transports across the sections may be computed from the mean salinities:

$$T_3(23.61) + (355 - T_3)(31.2) = 355(26.55) \tag{14}$$

$$T_1(27.49) + (355 - T_1)(31.2) = 355(26.55) \tag{15}$$

The transport at Section 2 is the actual observed transport. The mean and surface velocities are calculated from the cross-sections and transports.

$$v_m = \frac{\Sigma\, T}{\Sigma\, A} \tag{16}$$

$$v_s = 2.5\, v_m \tag{17}$$

The various values are presented in Table 8 B.

We note that the salinity profile remains unaltered as we proceed along the bay. The effect of turbulence at the boundary will be to mix

TABLE 8 A

Mean Salinities at Sections 1, 2 and 3

July

z (m)	$\bar{v}_z/\bar{v}_s$	A ($m^2 \times 10^2$)	$T/\bar{v}$ (m^2)	S (°/oo)	$S\,t/\bar{v}$ (°/oo m^2)	S_m
Section 1:						
0	1.00	4.3	430	22.8	98	
1	0.68	8.6	585	27.0	158	
2	0.47	8.6	404	30.10	122	
3	0.26	8.5	221	30.40	67	
4	0.16	8.5	136	30.68	42	
5	0.05	8.5	43	30.74	13	
		$\Sigma\, T/\bar{v}$ = 1819		$\Sigma\, sT/\bar{v}$ = 500		27.49 °/oo
Section 2:						
0	1.00	4.5	450	20.8	94	
1	0.68	8.9	605	25.5	154	
2	0.47	8.9	418	30.02	126	
3	0.26	8.8	229	30.30	70	
4	0.16	8.8	141	30.66	43	
5	0.05	8.8	44	30.71	14	
		$\Sigma\, T/\bar{v}$ = 1887		$\Sigma\, sT/\bar{v}$ = 501		26.55 °/oo
Section 3:						
0	1.00	4.5	450	16.8	76	
1	0.68	8.9	605	19.6	119	
2	0.47	8.9	418	29.89	125	
3	0.26	8.9	231	30.20	70	
4	0.16	8.8	141	30.63	43	
5	0.05	8.8	44	30.68	13	
		$\Sigma\, T/\bar{v}$ = 1889		$\Sigma\, sT/\bar{v}$ = 443		23.61 °/oo

some of the fresh water downward. Thus the actual upward flux of salt will be somewhat greater than the indicated by the actual salinity at the level of no net motion. A salinity value of 31.2 °/oo was chosen as most reasonable.

TABLE 8 B

Values of Transport, Salinity, and Velocity at Sections 1, 2, and 3

July

Section	Mean Salinity °/oo	Transport $m^3\ sec^{-1}$	Cross-Section m^2	Mean Velocity $cm\ sec^{-1}$	V_s $cm\ sec^{-1}$
1	27.49	445	4700	9.5	24
2	26.55	355	4900	7.2	18
3	23.61	217	4880	4.4	12

To evaluate $\bar{v}_x \frac{\partial \bar{v}_x}{\partial x}$ for Section 2 intermediate between Section 1 and Section 3, it was assumed that the ratio of a velocity at a given depth to the surface velocity was the same at all three sections. Then for Section 2:

$$\bar{v}_x \frac{\partial \bar{v}_x}{\partial x} = \frac{1}{2} \frac{\partial \bar{v}_x^2}{\partial x}$$

$$= \frac{1}{2} \frac{\left(\bar{v}_{x,1}^2 - \bar{v}_{x,3}^2 \right)}{\delta_x}$$

substituting

$$\bar{v}_{x,1} = 9.5/7.2\ \bar{v}_{x,2}$$

$$\bar{v}_{x,3} = 4.4/7.2\ \bar{v}_{x,2}$$

$$\bar{v}_x \frac{\partial \bar{v}_x}{\partial x} = 0.69\ \frac{\bar{v}_{x,2}^2}{\delta_x}$$

Substitution of $\delta x = 1.5 \times 10^5$ cm in the above equation gives:

$$\bar{v}_x \frac{\partial \bar{v}_x}{\partial x} = 0.46 \bar{v}_{x,2}^2 \times 10^{-5} \tag{18}$$

Equation (18) was used to evaluate $\bar{v}_x \frac{\partial \bar{v}_x}{\partial x}$ for the first 5 meters at Section 2. The results are shown in Table 9.

The 220 m^3 sec^{-1} added to the upper layer are advected from the middle layer with deceleration of the incoming water. The observed transport into the bay was measured at Section 2 at 380 m^3 sec^{-1}. This gives, as the most reasonable estimated values, a transport into the bay between 5 and 30 meters of 470 m^3 sec^{-1} at section 1, and of 240 m^3 sec^{-1} at Section 3. It is considered that there is negligible exchange between this layer and the water below 30 meters in the traverse from Section 1 to 3. Since all the inflowing water is sensibly homogeneous as to salinity, the ratio of transports must apply to the ratio of velocities; similarly, to the derivation of Equation (18):

$$\frac{\partial \bar{v}_x}{\partial x} = \frac{\bar{v}_{x,1} - \bar{v}_{x,3}}{\delta_x} = 0.44 \bar{v}_{x,2} \times 10^{-5}$$

$$\bar{v}_x \frac{\partial \bar{v}_x}{\partial x} = 0.44 \bar{v}_{x,2}^2 \times 10^{-5} \tag{19}$$

Values of $\bar{v}_x \frac{\partial \bar{v}_x}{\partial x}$, using Equation (19), from 5 to 35 meters are given in Table 9.

$\bar{v}_x \frac{\partial \bar{v}_x}{\partial x}$ is negligible below 30 meters. Velocities are very low, and the gradients are also much less than those existing in the upper layers. Small deceleration of the outgoing water, as might be anticipated from either continuity or advection, is negligible.

TABLE 9

Evaluation of $\bar{v}_x \frac{\partial \bar{v}_x}{\partial x}$ for July Conditions

z (m)	$\bar{v}_x$ (m $sec^{-1} x10^2$)	$\bar{v}_x \frac{\partial \bar{v}_x}{\partial x}$ (cm $sec^{-2} x10^5$)
0	18	150
1	14	90
2	9	37
3	6	17
4	3	4
5	1	0
6	- 0.5	0
7	- 2	2
8	- 3	4
9	- 4	7
10	- 5	11
15	- 3	5
20	- 1.5	2
25	- 0.5	0
30	0	0
35	0	0

4.5 Evaluation of $\bar{v}_x \frac{\partial \bar{v}_x}{\partial x}$ in March

The upper, outflowing layer in March is relatively deep, about 30 meters. Acceleration of this layer, as required by the salt balance for the entire layer, is small and the mean value of $\bar{v}_x \frac{\partial \bar{v}_x}{\partial x}$ for the layer would be negligible were it not for the fact that virtually all of the dilution of the salt occurs in the upper 5 meters by advective processes with consequent acceleration. A few serial observations of drift-sticks and poles enabled direct estimation of $\bar{v}_x \frac{\partial \bar{v}_x}{\partial x}$. Values were also obtained using the same procedure as in Paragraph 4.4. Values of $\bar{v}_x \frac{\partial \bar{v}_x}{\partial x}$ as obtained by both methods are reported in Table 10. The average of the two was taken as the accepted value.

TABLE 10

Evaluation of $\bar{v}_x \frac{\partial \bar{v}_x}{\partial x}$ for March Conditions

z (m)	$\bar{v}_x$ (cm sec^{-1})	Measured $\bar{v}_x \frac{\partial \bar{v}_x}{\partial x}$ (cm $sec^{-2} \times 10^5$)	Salt Cont. $\bar{v}_x \frac{\partial \bar{v}_x}{\partial x}$ (cm $sec^{-2} \times 10^5$)	Av. $\bar{v}_x \frac{\partial \bar{v}_x}{\partial x}$ (cm $sec^{-2} \times 10^5$)
0	12	20	17	18
1	9	10	8	9
2	6	5	3	4
3	4	1	1	1
4	3	0	0	0
5	2	0	0	0

Below 10 meters, the values of $\bar{v}_x$ are small and no significant values of $\bar{v}_x \frac{\partial \bar{v}_x}{\partial x}$ are found. Since inflow in March extends to the bottom, some acceleration may be expected in the bottom layer as it approaches the sill at Section 3 because of the smaller cross sectional area. These accelerations, all small, are computed on the basis of continuity requirements, and are included in Table 11.

4.6 Evaluation of $\bar{v}_z \frac{\partial \bar{v}_x}{\partial z}$ in July

The imposition of continuity requires that the 228 m^3 sec^{-1} added to the upper layer be transported across the 5-meter surface, and enables an evaluation of a mean vertical velocity at that depth. A typical tabulation would be:

Area of 5-meter surface	12.8×10^5 m^2
Transport through 5-meter surface	228 m^3 sec^{-1}
Mean vertical velocity at 5 meters	- 0.018 cm sec^{-1}

Similar computation of v_z has been made for various depths. The values are reported in Table 11.

The value of $\bar{v}_z$ must be zero at the surface, negative immediately beneath the surface. Below 20 meters, both $\bar{v}_z$ and $\frac{\partial \bar{v}_x}{\partial z}$ become very small, and there is no appreciable contribution to $\bar{v}_z \frac{\partial \bar{v}_x}{\partial z}$ below 20 meters. Values of $\bar{v}_z \frac{\partial \bar{v}_x}{\partial z}$ are also reported in Table 11.

TABLE 11

Evaluation of $\bar{v}_z \frac{\partial \bar{v}_x}{\partial z}$ for July Conditions

z	$\Delta_x \bar{v}_x$	$\Delta_z A_x$	$\Delta_x T$	$\Sigma \Delta_x T$	$\Delta_z A_y$	$\bar{v}_z$	$\frac{\partial \bar{v}_x}{\partial z}$	$\bar{v}_z \frac{\partial \bar{v}_x}{\partial z}$
(m)	(m $sec^{-1} \times 10^2$)	($m^2 \times 10^{-1}$)	(m^3 sec^{-1})	($m^2 \times 10^{-4}$)		(cm sec^{-1})	(sec^{-1})	(cm $sec^{-2} \times 10^5$)
0	12.5	45	56			0	-	0
				36	130	-0.005		
1	8.5	89	75			-0.007	-0.05	35
				131	130	-0.010		
2	5.5	89	50			-0.013	-0.04	52
				181	129	-0.014		
3	3.5	89	32			-0.015	-0.03	45
				213	129	-0.016		
4	1.5	88	13			-0.017	-0.02	34
				226	128	-0.018		
5	0	196	0			-0.018	-0.015	27
				226	126	-0.017		
8	-1.5	215	-33			-0.016	-0.010	15
				193	124	-0.015		
10	-3.0	255	-77			-0.014	0.00	0
				116	121	-0.010		
15	-1.5	412	-62			-0.008	0.003	-2
				54	117	-0.005		
20	-1.0	400	-40			-0.003	0.001	0
				14	114	-0.001		
25	-0.2	385	- 8			-0.001	0.001	0
				6	108	-0.000		
30	0	370	0			0	0	0

4.7 Evaluation of $\bar{v}_z \frac{\partial \bar{v}_x}{\partial z}$ in March

$\bar{v}_z \frac{\partial \bar{v}_x}{\partial z}$ was much smaller in March than in July. On the assumption that in March advection proceeds from the bottom to the top layer at a more or less constant rate along the channel, the value of $\bar{v}_z \frac{\partial \bar{v}_x}{\partial z}$ may be computed across the depth of no net horizontal motion as before.

Area of 30-meter surface	10.2×10^5 m^2
Estimated transport through surface	100 m^3 sec^{-1}
Mean vertical velocity at 30 meters	- 0.009 cm sec^{-1}

The value of the velocity gradient, $\frac{\partial \bar{v}_x}{\partial z}$, is approximately 0.0008 sec^{-1}. The resulting value for $\bar{v}_z \frac{\partial \bar{v}_x}{\partial z}$ is 7×10^{-6}, which is negligible compared to the value of the other terms in the equation. The values chosen above were chosen as maximum estimates, and since both $\bar{v}_z$ and $\frac{\partial \bar{v}_x}{\partial z}$ decrease in magnitude away from the 30-meter surface, there is no appreciable contribution from this term except near the surface where the velocity gradient, $\frac{\partial \bar{v}_x}{\partial z}$, again increases. If we assume maximum conditions, we may estimate the transport through the 5-meter surface as about 50 m^3 sec^{-1}. Since $\frac{\partial \bar{v}_x}{\partial z}$ is again very small below 5 meters, only the values of $\bar{v}_z \frac{\partial \bar{v}_x}{\partial z}$ above 5 meters are calculated. Values of both $\bar{v}_z$ and $\bar{v}_z \frac{\partial \bar{v}_x}{\partial z}$ are given in Table 12.

4.8 Consideration of $\left\langle \frac{1}{\rho} \frac{\partial p}{\partial y} \right\rangle$

Equation (7) is differentiated with respect to the y-coordinate:

$$\frac{\partial \bar{p}}{\partial y} = g \rho_s \frac{d\zeta}{dy} + g \int_0^z \frac{\partial \rho}{\partial y} dz \tag{20}$$

Equation (20) is now substituted into equation (4)

$$g \frac{\rho_s}{\rho} \frac{d\zeta}{dy} + \frac{g}{\rho} \int_0^z \frac{\partial \rho}{\partial y} dz - f \bar{v}_x + Y = 0 \tag{21}$$

The value of the Coriolis parameter, f, is 1.2 x 10^{-4} sec^{-1} at Silver Bay. Insufficient lateral stations were obtained during the summer (July) survey to determine the lateral pressure gradients. For March, there are, in general, no series of measurements at depths greater than 30 meters. The terms in the y-equation of motion apparently are an order of magnitude smaller than the ones in the x-equation. Accuracy of determinations does not appear sufficient to calculate a balance for these terms.

TABLE 12

Evaluation of $\bar{v}_z \frac{\partial \bar{v}_x}{\partial z}$

z	$\Delta_z \bar{v}_x$	$\Delta_z A_x$	$\Delta_z T$	$\Sigma\Delta T$	ΔA_y	$\bar{v}_z$	$\frac{\partial \bar{v}_x}{\partial z}$	$\bar{v}_z \frac{\partial \bar{v}_x}{\partial z}$
(m)	(m sec^{-1} x10^2)	(m^2x10^{-1})	($m^3 sec^{-1}$)		(m^2x10^4)	(cm sec^{-1})	(sec^{-1})	(cm sec^{-2}x10^5)
0	2	45	9			0	-	0
				9	130	- 0.001	- 0.03	
1	2	89	18			- 0.001	- 0.03	3
				27	130	- 0.002		
2	1	89	9			- 0.002	- 0.025	5
				36	129	- 0.003		
3	1	89	9			- 0.003	- 0.015	4
				45	129	- 0.004		
4	0	88	0			- 0.004	- 0.010	4
				45	128	- 0.004		
5	0	88	0			- 0.004	- 0.005	2
				45	127	- 0.004		
6	0	87				- 0.004	0	0

CHAPTER 5

SALT BALANCE AND TRANSPORT

5.1 Purpose of Study of Salt Balance

A study of the salt balance in Silver Bay furnishes additional information about turbulent processes. The degree of success in satisfying the salt balance equations is, at least in part, a check of the consistency of the basic equations and the analysis of the data.

5.2 The Salt Balance

Because of the nature of the observations available, it is convenient to study the salt balance in segments extending across the estuary at its mouth. These segments are bounded by Sections 1 and 3, by the bottom and sides of the estuary, and by a top surface of varying depth (Figure 12).

Neglecting molecular diffusion, the instantaneous local rate of change of the salt concentration, s, is given by:

$$\frac{\partial s}{\partial t} = - \frac{\partial (v_i \, s)}{\partial x_i} \tag{22}$$

Designating the total salt content within the segment by $S = \iiint s \, dV$, where V is the volume of the segment, we have, using Equation (22):

$$\frac{\partial S}{\partial t} = \frac{\partial}{\partial t} \left\{ \iiint_V s \, dV \right\} = - \iiint \frac{\partial}{\partial x_i} (v_i s) \, dV \tag{23}$$

Applying Green's theorem to Equation (23):

$$\frac{\partial S}{\partial t} = - \iint_\sigma (v_i s) \, d\sigma_i \tag{24}$$

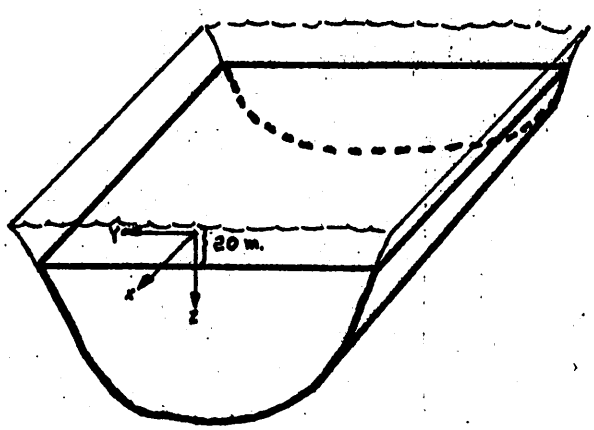

Figure 12. Typical segment, z = 20 m., used for salt balance.

Where $\iint d\sigma_i$ now represents the integral over the bounding surfaces of the segment. Now introducing into Equation (24), for the instantaneous velocity and salinity, sums of a mean term and a random term, and taking the time mean of the resulting equation, we obtain:

$$\left\langle \frac{\partial S}{\partial t} \right\rangle = - \iint_\sigma \langle v_i' S' \rangle \, d\sigma_i - \iint_\sigma \bar{v}_i \bar{s} \, d\sigma_i \tag{25}$$

Applying Equation (24) to the specific segment bounded by Sections 1 and 3, bottom, sides and surface of the channel, and considering, $\left\langle \frac{\partial S}{\partial t} \right\rangle$, as negligible in accord with observation, equation (24) becomes:

$$\iint_{\sigma_x} \bar{v}_x \bar{s} \, d\sigma_x + \iint_{\sigma_x} \langle v_x' s' \rangle \, d\sigma_x = 0 \tag{26}$$

The first term of Equation (26) may be considered in two parts: first, the integral in the upper outflowing layer where $\bar{v}_x$ is positive; and second, the integral over the lower inflowing layer where $\bar{v}_x$ is negative. $\iint_{\sigma_x} \bar{v}_x \bar{s} \, d\sigma_x$ has been evaluated in Table 13 and Table 14 for March and July conditions respectively. The value of the integral $\iint_{\sigma_x} \langle v_x' s' \rangle d\sigma_x$ as determined from Equation (26) is less than 10 percent of either of the two parts of the first term of Equation (26) for both summer and winter conditions. This means that the salinity balance within a segment bounded by the surface and the bottom is maintained primarily by horizontal advection, the horizontal diffusion being of only slight importance. In the evaluations which follow, horizontal diffusion will thus not be considered.

Because of the manner in which the segments were chosen, neither lateral advection nor diffusion will enter into consideration of the salt balance on the assumption of negligible horizontal diffusion, and

TABLE 13

Salt Balance in March

z	$\bar{v}_{x,1}\bar{s}_1$	$\bar{v}_{x,2}\bar{s}_2$	$\Delta\bar{v}_x\bar{s}\,\delta\sigma_x$	$\iint\sigma\bar{v}_x\bar{s}\,d\sigma_z$	$\bar{v}_z\bar{s}\sigma_z$	$\langle v_z's'\rangle\sigma_z$
(m)	(gm cm^{-2} sec^{-1}x10)		(gm sec^{-1}x10^8)			
				0.1		
0	39.1	32.4	6.0			
				5.9	6	- 0.1
2	20.1	17.0	5.5			
				11.4	12	- 0.6
4	8.8	7.2	2.8			
				14.2	14	0.2
6	5.3	4.3	1.7			
				15.9	16	- 0.1
8	5.3	4.3	1.7			
				17.6	18	- 0.4
10	7.0	5.8	4.0			
				21.6	21	0.6
15	6.5	5.4	4.1			
				25.7	24	1.7
20	5.3	4.3	4.0			
				29.7	27	2.7
25	2.1	1.7	1.5			
				31.2	30	1.2
30	0	0	0			
				31.2	30	1.2
35	- 3.5	- 2.8	- 2.1			
				29.1	28	1.1
40	- 4.6	- 3.8	- 2.6			
				26.5	26	0.5
45	- 5.3	- 4.3	- 3.2			
				23.3	23	0.3
50	- 6.4	- 5.2	- 3.7			
				19.6	19	0.6
55	- 6.7	- 5.5	- 3.7			
				15.9	15	0.9
60	- 6.7	- 5.5	- 3.6			
				12.3	13	- 0.7
65	- 6.4	- 5.2	- 3.6			
				8.7	9	- 0.3
70	- 5.3	- 4.3	- 2.9			
				5.8	6.0	- 0.2
75	- 4.6	- 3.8	- 2.3			
				3.5	4.0	- 0.5
80	- 3.5	- 2.9	- 1.7			
				1.8	2.0	- 0.2
85	- 2.1	- 1.7	- 1.1			
				0.7	0.8	- 0.1
90	- 1.1	- 0.9	- 0.5			
				0.2	0.3	- 0.1
95	- 0.4	- 0.3	- 0.2			
				0	0	0
100	0	0	0			

TABLE 14

Salt Balance in July

z	$\bar{v}_{x,1}\bar{s}_1$	$\bar{v}_{x,2}\bar{s}_2$	$\Delta\bar{v}_x\bar{s}\,\delta\sigma_x$	$\iint_\sigma \bar{v}_x\bar{s}\,d\sigma_x$	$\bar{v}_z\bar{s}\,\sigma_x$	$\langle v_z's'\rangle\sigma_z$
(m)	(gm cm^{-2} sec^{-1}x10)		(gm sec^{-1}x10^8)			
				- 0.2		
0	49.6	17.8	- 14.3			
				14.1	12.4	1.7
1	-	-	- 21.1			
				35.2	33.5	1.7
2	31.6	15.2	- 14.6			
				49.8	52.1	-
3	-	-	- 8.4			
				58.2	60.4	-
4	11.1	5.4	- 5.0			
				63.2	64.8	-
5	3.2	1.5	- 1.5			
				64.7	64.5	0.2
6	- 1.2	- 1.6	1.5			
				64.2	63.1	1.1
7	- 5.8	- 3.7	1.8			
				62.4	60.5	1.9
8	- 10.1	- 6.2	3.4			
				59.0	58.5	0.5
9	- 14.2	- 8.7	4.7			
				54.3	51.3	2.5
10	- 20.4	-12.8	19.0			
				35.3	36.1	- 0.8
15	- 12.4	- 7.6	19.3			
				16.0	15.2	0.8
20	- 6.1	- 3.8	9.2			
				6.8	6.0	0.8
25	- 3.6	- 2.2	5.3			
				1.5	1.3	0.2
30	- 1.0	- 0.6	1.5			
				0	0	
35	0	0	0			

leaving $\left\langle \frac{\partial S}{\partial t} \right\rangle$ in the equation, Equation (25) may be evaluated for a segment whose upper surface lies at depth h as:

$$\left\langle \frac{\partial S}{\partial t} \right\rangle = - \iint_{\sigma_h} \bar{v}_x \bar{s} \; \sigma_x - \langle v'_h s' \rangle \sigma_h - \bar{v}_h \bar{s} \sigma_h \qquad (27)$$

Equation (27) is evaluated in Tables 13 and 14 for March and July conditions. The values of $\bar{v}_x$s and $\bar{v}_z$s are taken from the observed mean values. $\left\langle \frac{\partial S}{\partial t} \right\rangle$ was computed from the change observed in the mean salinity of the segment between the time of the initial and final observations of the surveys. The effect of random advection was so strong as to make impossible an estimate in the value of $\left\langle \frac{\partial S}{\partial t} \right\rangle$ in the upper layer in July. In the lower layer below 25 meters a general decrease of salinity of 0.08 °/oo was observed in a $5\frac{1}{2}$-day period. The volume of the segment below 35 meters (refer to Figure 12) is 6.1×10^7 m^3. This represents a value of $\left\langle \frac{\partial S}{\partial t} \right\rangle$ of 11,000 g sec^{-1}. This figure is possibly related to slight currents below the range of the metering devices, or to diffusion. The value is so small compared to the large advective changes as to be masked by the effects in the surface layer. No appreciable local salt change was observed in March. Hence, no values for $\left\langle \frac{\partial S}{\partial t} \right\rangle$ are reported in Table 13 and Table 14.

The integral to be evaluated in Equation (27) is a surface integral. $\bar{v}_x \bar{s}$ is evaluated over the two sections at the end of the segment and $\bar{v}_z \bar{s}$ over the top surface of the segment. The column headed $\Delta \bar{v}_x \bar{s} \; \delta\sigma_x$ represents $\left(\bar{v}_x \bar{s} \Big]_{\sigma 1} - \bar{v}_x \bar{s} \Big]_{\sigma 2} \right) \delta\sigma_x$, the net value of $\Delta \bar{v}_x \bar{s}$ evaluated over the surface $\delta\sigma_x$. Since progressive segments are added onto the top, summation proceeds from the bottom upwards, beginning at the level 35 m, where the term $\Delta \bar{v}_x \bar{s} \; \delta\sigma_x$ becomes of appreciable size. No physical reality

is implied in reporting negative values of $\langle v_z' s' \rangle \sigma_z$. They are related to range of error in the large advective terms.

It can be seen that the salt balance in Silver Bay primarily is due to a balance of horizontal and vertical advection, with the vertical eddy diffusion of secondary or negligible importance.

5.3 Transport

The volume transport of water through cross-section 2 has been computed for both March and July conditions. The results are presented in Table 15. Values are computed from the bathymetric chart. Very small mean velocities made it difficult to accurately establish the velocity profile for July in the lower layers. The reported transports for depths below 30 meters in July are chosen to match the observed changes in water properties within Silver Bay at these levels, and to provide the balance between the better defined transports observed in the upper layers. In this sense, the transports below 30 meters are inferred, and not based on direct measurements, but are supported by the direct measurements available.

5.4 Eddy Coefficients

Eddy coefficients are computed from the values of $\langle v_x' v_z' \rangle$ already obtained. The relations used were the common ones:

$$\langle v_z' v_x' \rangle = -\rho N_z \frac{\partial \bar{v}_x}{\partial z}$$

TABLE 15

Observed Transport

z (m)	A (m^2 x 10^2)	$\bar{v}_x$ July (cm sec^{-1})	T July (m^3 sec^{-1})	$\bar{v}_x$ March (cm sec^{-1})	T March (m^3 sec^{-1})
0	9.0	16	144	10	90
1	8.9	11	98	7	62
2	8.8	7	62	4	35
3	8.8	4	35	3	26
4	8.8	2	18	2.5	22
5	8.7	0	0	2	17
6	8.7	- 1	- 9	1.5	13
7	8.6	- 2	- 17	1.5	13
8	8.6	- 3	- 26	1.6	14
9	8.5	- 4	- 34	1.8	15
10	41.7	- 4	- 167	2	18
15	40.5	- 2	- 81	1.8	73
20	39.2	- 1	- 39	1.2	47
25	37.7	- 0.5	- 19	0.1	4
30	36.0	0	- 0	- 0.8	- 29
35	34.2	0	- 0	- 1.2	- 41
40	33.0	0	- 0	- 1.4	- 46
45	32.5	0	- 0	- 1.6	- 52
50	31.5	0	- 0	- 1.8	- 57
55	31.0	0.1	- 3	- 2.0	- 62

(continued)

TABLE 15 (continued)

z (m)	A ($m^2 \times 10^2$)	$\bar{v}_x$ July (cm sec^{-1})	T July (m^3 sec^{-1})	$\bar{v}_x$ March (cm sec^{-1})	T March (m^3 sec^{-1})
60					
	30.2	0.2	6	- 1.9	- 57
65					
	29.7	0.2	6	- 1.7	- 50
70					
	29.2	0.2	6	- 1.4	- 41
75					
	28.7	0.3	9	- 1.2	- 34
80					
	28.0	0.4	11	- 0.8	- 22
85					
	27.0	0.5	14	- 0.4	- 11
90					
	25.5	0.5	13	- 0.2	- 5
95					
	23.0	0.4	9	0	0
100					
	17.0	0.3	5	0	0
105					
	8.0	0.1	1	0	0
110 Bottom					

TABLE 16

Eddy Coefficients

Investigator	Location	Representative values of N_z (in cm^2 sec^{-1})
Jacobsen	Kattegat	0.9 - 2.4
Trites	British Columbia Inlets	0.1 - 10
Pritchard	James River	1.5 - 6
McAlister et. al.	Silver Bay, July	3 - 30
McAlister et. al.	Silver Bay, March	5 - 120

Some of the values are quite large, representative of the high rate of turbulent mixing in this region. For purposes of comparison, values are included in Table 16 of eddy coefficients determined by Jacobsen (1913) in the Kattegat; Pritchard (1956) in Chesapeake Bay; and Trites (1955) in British Columbia inlets.

CHAPTER 6

DISCUSSION AND CONCLUSIONS

6.1 The Velocity Field

The vertical velocity profiles (Figures 9 and 10) were determined directly from the current measurements, except that the section of the July profile below 30 meters is drawn so as to conform best to the observed change in water properties in the inlet, and to provide the necessary transport. No velocity measurements were obtained at depth in July which would not support the accepted curve.

No attempt was made to calculate lateral velocities as there is no evidence of the existence of a lateral circulation in Silver Bay. The current measurements appear to show a random variation about the two preferred directions -- directly into, and out from the channel -- and the assumption of a zero mean lateral velocity appears justified.

The difference in shape of the two curves indicates a difference in the type of circulation prevailing in Silver Bay at the time of the two measurements. The July circulation was largely driven by the addition of fresh water into the inlet; while the March circulation appears to be caused largely by the replacement of water at depth in Silver Bay.

6.2 The Stress Field

The vertical distribution of stress, $\langle v_x' \, v_z' \rangle$ (Figures 13 and 14) was computed by integration of the corresponding values of $\frac{\partial}{\partial z} \langle v_x' \, v_z' \rangle$ from Tables 4 and 5. The integration proceeds upwards from the bottom, since the major uncertainties in measurement appear in the

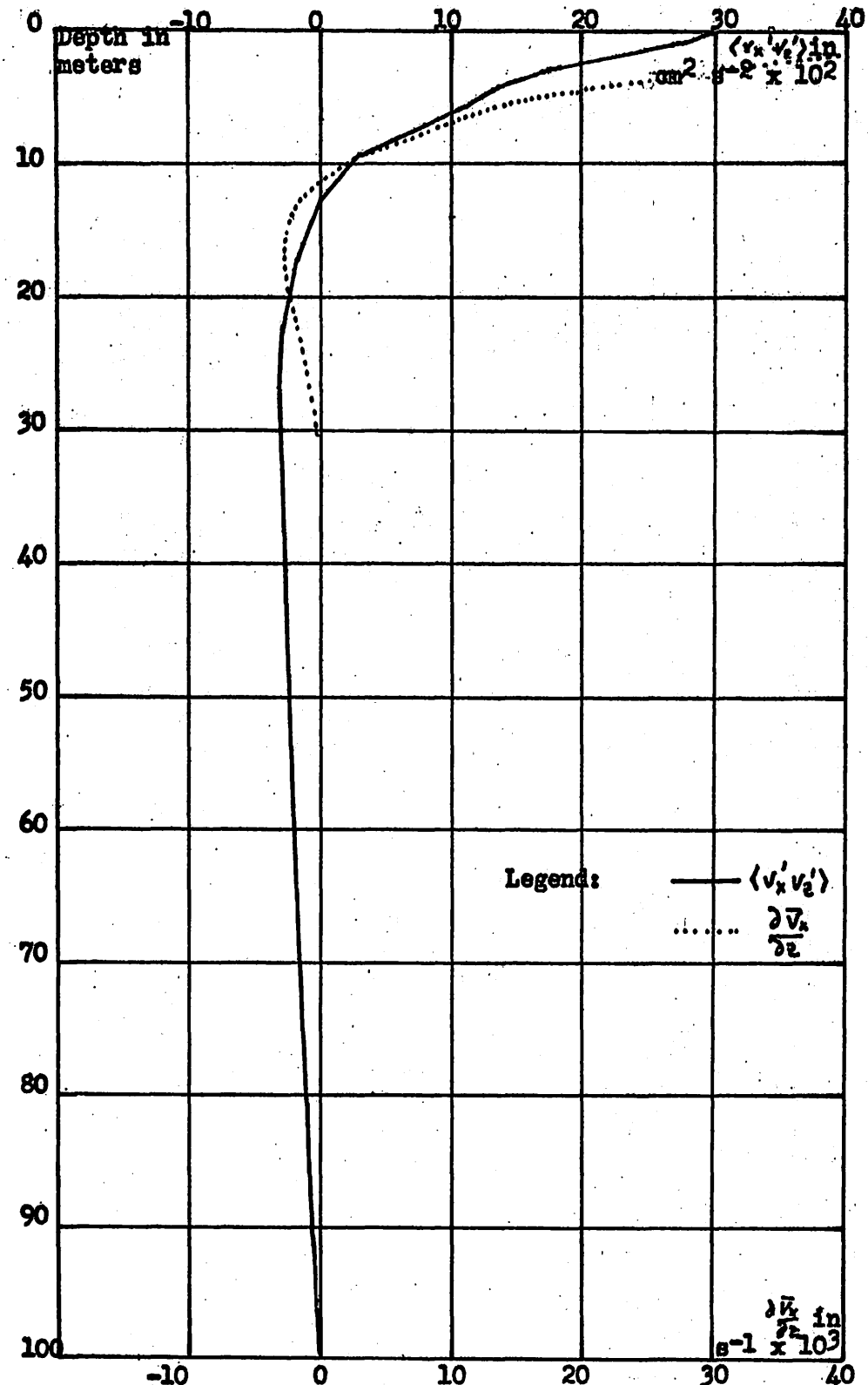

Figure 13. Variation of $\langle v_x' v_z' \rangle$ and $\frac{\partial \bar{v}_x}{\partial z}$ with Depth, July

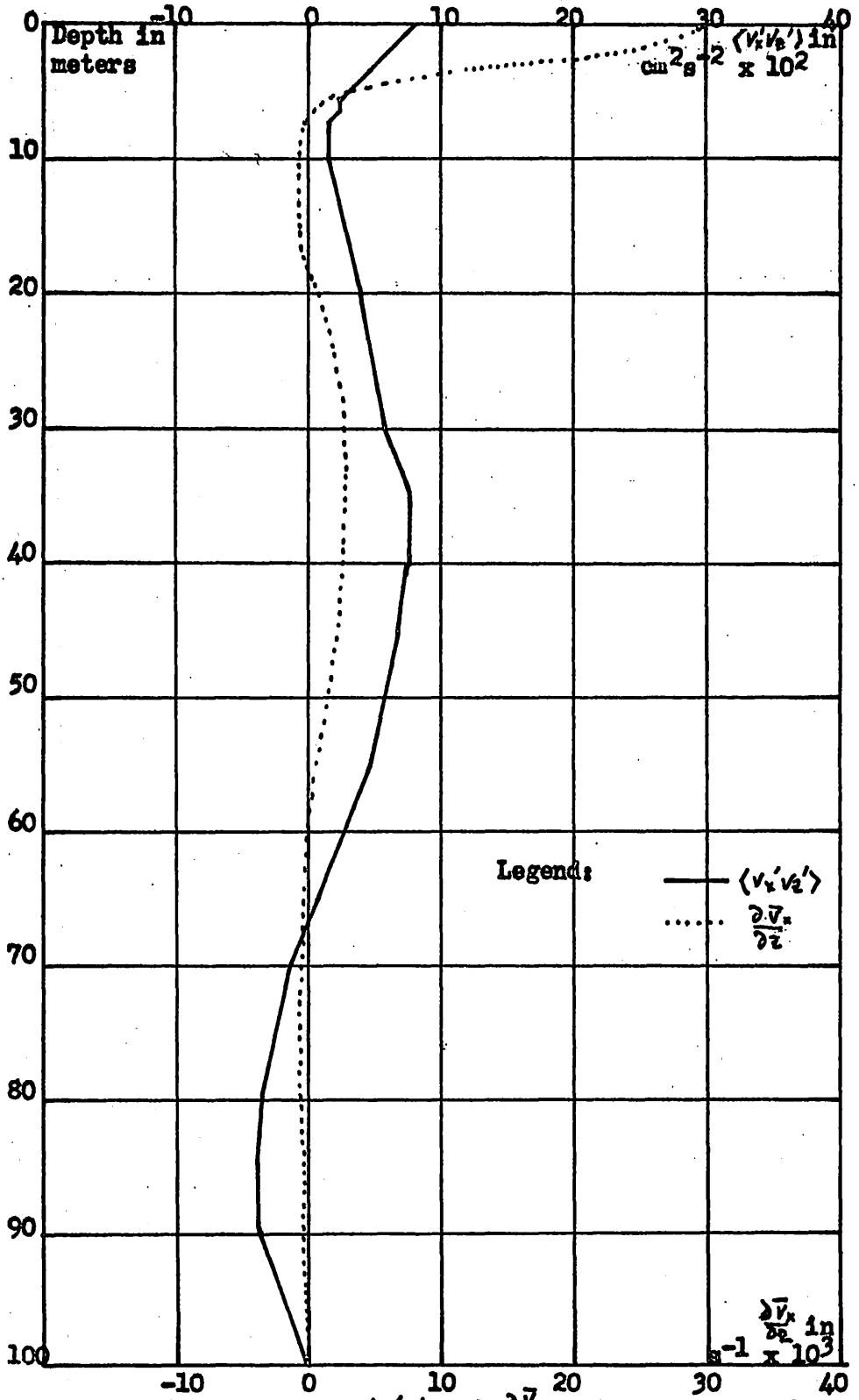

Figure14. Variation of $\overline{(v_x'v_z')}$ and $\frac{\partial \bar{v}_x}{\partial z}$ with Depth, March

upper few meters. The values obtained in this manner for the surface stress agree with the value for the surface stress as computed for the mean wind.

6.3 The Pressure Gradient, Stress Gradient, and Intertial Fields

These are the fields which constitute the solution of the equations of motion given in Tables 4 and 5. The various fields are shown in Figures 15 and 16.

In both cases, winter and summer, there is a strong pressure gradient at the surface associated with the surface slope. The large gradient is limited to the upper 5 meters. In the winter there is a level pressure surface approximately associated with the level of no net motion. Below this level the circulation consists of a balance between the pressure gradient and the vertical stress gradient. In the summer the pressure field never reverses and, even for the inflowing layer, the pressure is greater inside Silver Bay than outside. This requires that some mechanism which will accelerate the inflowing water must exist seaward of the sections at which the measurements were taken.

It is not possible, from the observations available, to determine the forces acting outside the estuary mouth, but several possibilities may be mentioned. Pressure gradients in the area outside may be quite different from those within Silver Bay because of mixing of the water column, and because of possible pressures from Coriolis effects associated with cross-channel currents.

Another mechanism may be the sudden widening of the channel at the mouth oi Silver Bay. The general effect of such widening would be to

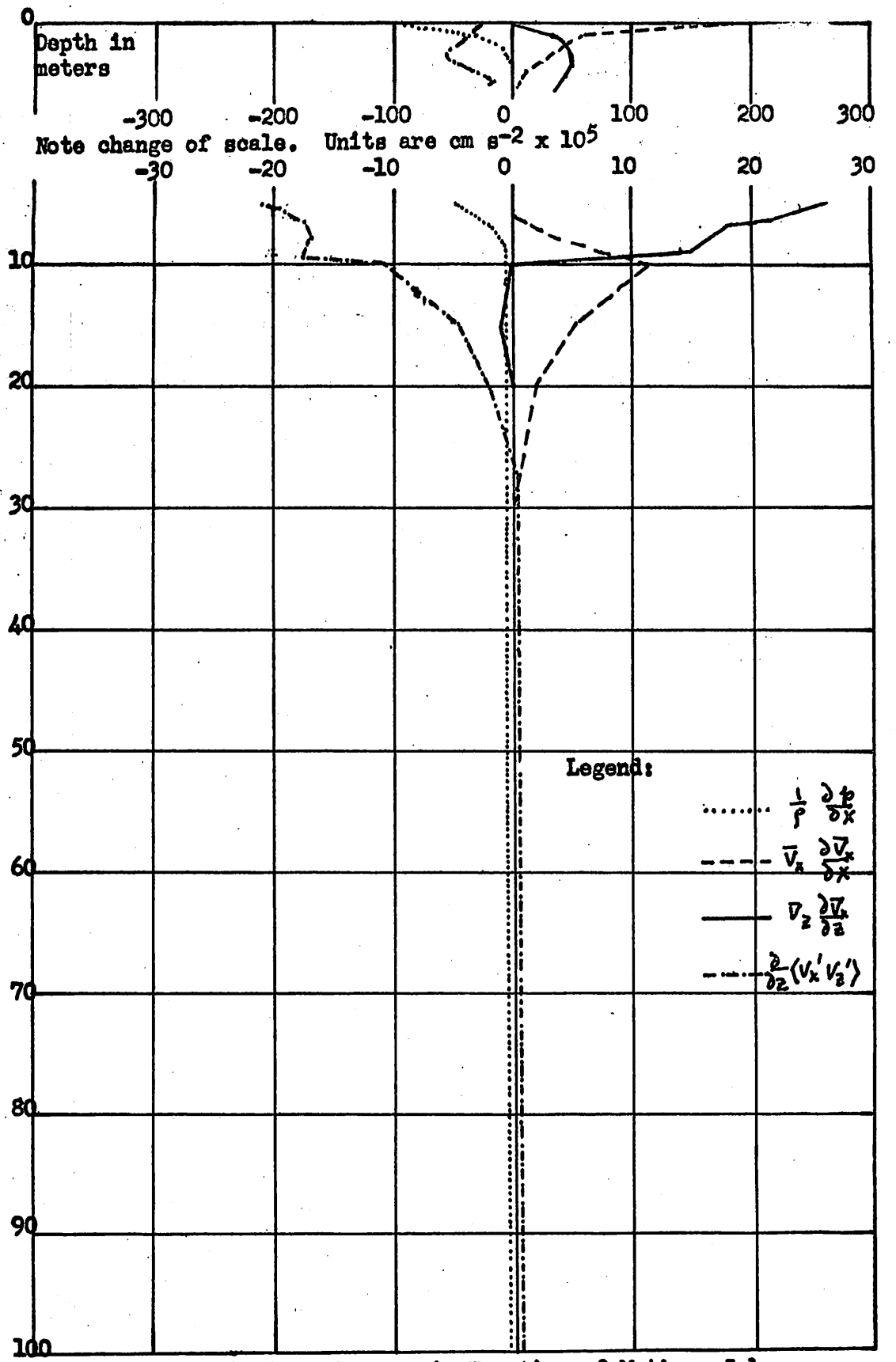

Figure 15. Variation of Terms in Equation of Motion, July

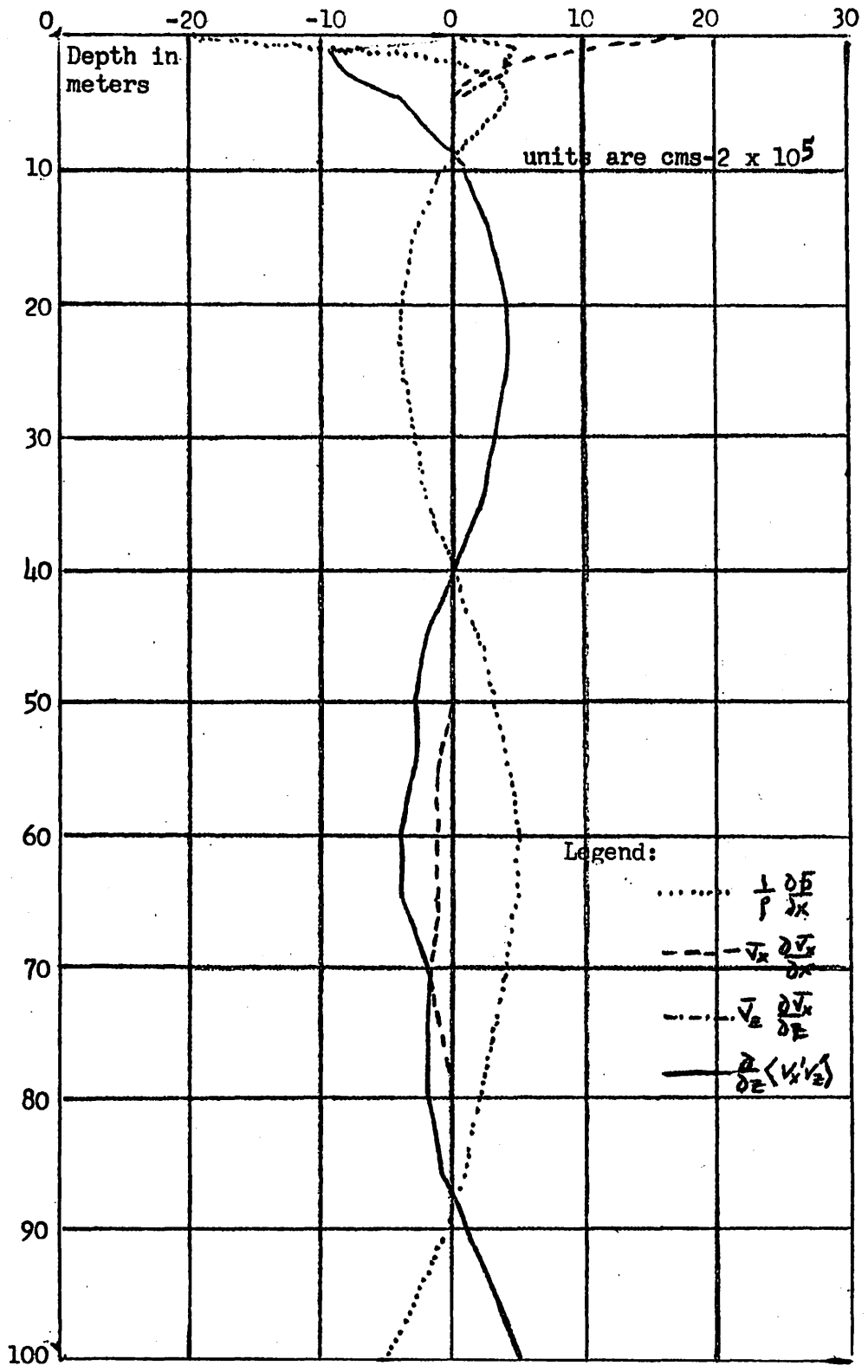

Figure 16. Variation of Terms in Equation of Motion, March

decrease the depth and velocity of the upper layer, and to accelerate the lower layer entering Silver Bay. However, there are insufficient observational data to adequately determine the magnitude of such effects.

The inertial fields, $\bar{v}_x \frac{\partial \bar{v}_x}{\partial x}$, and $\bar{v}_z \frac{\partial \bar{v}_x}{\partial z}$ are important in the upper faster moving layers of the system. This is a distinction from the case of the coastal plain estuary, where the only inertial term of significant value is the term associated with the tidal velocity, $U_o \frac{\partial U_o}{\partial x}$.

6.4 Comparison With Theory

There exist two expositions of theories of circulation in a fiord estuary, those of Stommel (1952) and of Cameron (1951). Stommel has considered a simple steady state fiord composed of two layers. The lower layer contains salt water of oceanic salinity, and the top layer is diluted, brackish water. From continuity considerations, Stommel derives relations similar to those which were used in Sections 4.4 and 4.6 in deriving mean longitudinal and mean vertical velocities for Silver Bay. Stommel then introduces a third equation on the longitudinal rate of change of momentum flux in the upper layer, the validity of which has been questioned (Pritchard 1952).

In deriving this relation, Stommel considers the advective flux of momentum into the upper layer, but neglects turbulent effects. The analysis of the Silver Bay data indicates that for high runoff conditions this is a reasonable assumption. The circulation observed in Silver Bay in July is well desribed by Stommel's theoretical model. Conditions in March, however, are not amenable to treatment by the theory. There is no

density discontinuity at the depth of no net motion, and the results of the theory in general, do not agree with observation.

Cameron (1951) combines the vertical and horizontal components of the equation of motion, and assumes a constant eddy coefficient of viscosity. He then introduces a stream-function, so chosen as to give a velocity profile similar to that obtained by Tully in Alberni Inlet (1949), and then proceeds to solve the resulting equation. The velocity profile obtained for Silver Bay in July using Cameron's equations and k = 0.1 agrees remarkably with the observed values. Since the velocity profile for Silver Bay in July is close to that obtained by Tully in Alberni Inlet, the result is probably to be expected. One result of Cameron's study is the concept of a critical velocity. The critical velocity for Silver Bay in July is 41 cm sec^{-1}. Observed surface velocities were about 50 percent of this value at the anchor station. At the observed rate of acceleration, the critical velocity would be exceeded slightly seaward of the mouth of the estuary.

The assumption of a constant eddy viscosity is not considered a strong restriction. As was mentioned previously, in typical July conditions, with the strong advective terms, the equations are relatively independent of assumptions about the nature of the eddy viscosity terms in the surface layers.

The system fails to explain the March regime, however. Neither velocity nor salinity profiles agree with prediction, and the observed surface velocity at the anchor station is already 120 percent of the critical velocity.

6.5 Conclusions

Sufficient reliable data were obtained in Silver Bay to permit the evaluation of the various terms in the equations of motion to an extent that the primary mechanics of the system are apparent and the system may be described in general.

The fresh water from stream or surface inflow overrides the saline water of the bay at its point of entrance. The accumulation of fresh water creates a pressure head, and the fresh water runs downhill towards the mouth of the bay. Two things happen to the surface water flowing out of the bay. As it flows out, essentially running downhill, it will accelerate and entrain salt water from the underlying saline water and become brackish. The effects of entrainment and acceleration balance to maintain a nearly uniform thickness of the surface layer along the channel. Since more water leaves the estuary as brackish water in this outflowing layer than enters the estuary as fresh water inflow, saline water must enter at a depth to maintain the volume of water in the bay. In the case of the July observations in Silver Bay, more water was entering the bay in this inflowing layer than was transported out at the surface, hence there was a small outflowing transport near the bottom.

The exact nature of the circulation with depth appears to depend not only upon the fresh water inflow, but upon the characteristics of the water masses already within the bay and in adjacent coastal waters; and upon the extent and nature of the circulation existing outside the mouth of the estuary. Such a determination has been beyond the scope of this study, limited to a description of the forces existing within the bay.

It is hoped that the evaluations presented here will further the understanding of the problems involved in the circulation and mixing of estuarine waters, and contribute to the general understanding of marine circulations.

REFERENCES

ARONS, A. B. and H. STOMMEL
1951. A mixing length theory of tidal flushing. Transactions American Geophysical Union, 32 (3): 419-421.

BARNES, CLIFFORD A., T. F. BUDINGER, E. E. COLLIAS, W. B. McALISTER, P. N. SUND, M. P. WENNEKENS
1956. Oceanography of Silver Bay. Special Report 24, University of Washington, Department of Oceanography.

CAMERON, W. M.
1951. On the dynamics of inlet circulations. Doctoral dissertation, University of California, Los Angeles, California.

KETCHUM, B. H.
1951. The exchanges of fresh and salt waters in tidal estuaries. Journal of Marine Research, 10 (1): 18-38.

PICKARD, G. L.
1953-1954. Oceanography of British Columbia Mainland inlets. Progress Reports Pacific Coast Stations, Numbers: 96, 97, 98, 99, Fisheries Research Board of Canada.

———. 1955. British Columbia inlets. Transactions American Geophysical Union, 36 (5): 897-901.

PRITCHARD, D. W.
1952. Estuarine hydrography. Advances in Geophysics, 1: 243-280.

———. 1954. A study of the salt balance in a coastal plain estuary. Journal of Marine Research, 13 (1): 133-144.

———. 1956. The dynamic structure of a coastal plain estuary. Journal of Marine Research, 15 (1): 33-42.

PROUDMAN, J.
1953. Dynamical oceanography. John Wiley and Sons, New York, 409 pages.

STOMMEL, H. and H. G. FARMER
1952. On the nature of estuarine circulation. Reference Numbers: 52-88, 52-51, 52-63, Woods Hole Oceanographic Institution.

SVERDRUP, H. U., M. W. JOHNSON, and R. H. FLEMING
1942. The Oceans. Prentice-Hall, Inc., New York, 1087 pages.

TRITES, R. W.
1955. A study of the oceanographic structure in British Columbia inlets and some of the determining factors. Doctoral dissertation, University of British Columbia, Vancouver, B. C.

TULLY, J. P.
1949. Oceanography and prediction of pulp mill pollution in Alberni inlet. Fisheries Research Board of Canada Bulletin 83, 169 pages.